AD NUMBER: AD0900245

LIMITATION CHANGES

TO:

Approved for public release; distribution is unlimited.

FROM:

Distribution authorized to U.S. Gov't. agencies only; Test and Evaluation Use; 04 JUN 1975. Other requests shall be referred to Air Force Avionics Laboratory, Wright-Patterson AFB, OH 45433.

AUTHORITY

AFAL ltr dtd 4 Jun 1975

AFAL-TR-72-5

LIGHTNING EFFECTS RELATING TO AIRCRAFT PART II - CHARACTERISTICS OF SIMULATED LIGHTNING FLASHES AND THEIR EFFECTS ON LIGHTNING ARRESTERS AND AVIONIC EQUIPMENT

F.A. Fisher
B. Macchiaroli
High Voltage Laboratory
General Electric Company

and

D. L. Jones
General Electric Company
Re-Entry & Environmental Systems Dept.

Technical Report AFAL-TR-72-5

January 1972

Air Force Avionics Laboratory
Air Force Systems Command
Wright-Patterson Air Force Base, Ohio

NOTICE

When Government drawings, specifications, or other data are used for any purpose other than in connection with a definitely related Government procurement operation, the United States Government thereby incurs no responsibility nor any obligation whatsoever; and the fact that the government may have formulated, furnished, or in any way supplied the said drawings, specifications, or other data, is not to be regarded by implication or otherwise as in any manner licensing the holder or any other person or corporation, or conveying any rights or permission to manufacture, use, or sell any patented invention that may in any way be related thereto.

Copies of this report should not be returned unless return is required by security considerations, contractual obligations, or notice on a specific document.

AFAL-TR-72-5

LIGHTNING EFFECTS RELATING TO AIRCRAFT PART II - CHARACTERISTICS OF SIMULATED LIGHTNING FLASHES AND THEIR EFFECTS ON LIGHTNING ARRESTERS AND AVIONIC EQUIPMENT

F.A. Fisher
B. Macchiaroli
High Voltage Laboratory
General Electric Company
and
D.L. Jones
General Electric Company
Re-Entry & Environmental Systems Dept.

Technical Report AFAL-TR-72-5

January 1972

Air Force Avionics Laboratory
Air Force Systems Command
Wright-Patterson Air Force Base, Ohio

FOREWORD

This document is Technical Report AFAL-TR-72-5, Part II and covers the Effects of Simulated Lightning Strokes on Lightning Arresters and Avionic Equipment and the Electrical Characters of Simulated Lightning Flashes. Part I covers Lightning Effects on Composite Materials and Electromagnetic Shielding Properties of Composite Materials. Part III covers simulated lightning tests on the F-4 aircraft avionics systems.

This Final Technical Report was prepared by General Electric Co. High Voltage Laboratory, Pittsfield MA in response to USAF contract F33615-70-C-1144. The contract was initiated under AFAL exploratory development project 4357 task 12 under the direction of Mr. H.M. Bartman, Project Engineer, AFAL/AAA and supported by Mr. Herbert Schwartz of the Air Force Materials Laboratory (AFML/LN).

The contractor's activity was under the direction of Mr. F.A. Fisher, Project Manager, assisted by L.C. Walko, B. Macchiaroli, D.B. McElhinny, and G.W. Maihl of General Electric and supported by W.M. Fassell, Project Manager, and J.W. McCamont of Philco Ford.

Technical Report AFAL-TR-72-5, Part II has been reviewed and is approved.

WILLIAM A. STUDABAKER
Lt Colonel, USAF
Chief, System Avionics Div
AF Avionics Laboratory

ABSTRACT

Measurements were made of the degree to which a lightning arrester could limit the voltage on avionic equipment when an external lightning arrester was struck by a simulated lightning stroke. The tests show that breakdown is not an instantaneous affair, but rather takes many microseconds. Measurements taken near a point which is struck indicate that the air around any protrusions will be in a state of electrical breakdown whenever the electrical field strength at the aircraft surface approaches 100 kV/Meter. Electrical discharges tend to limit the field strength to that value, thus defining the electrical environment to which the avionics equipment is subjected. Data is presented showing how the impedance affects the voltages impressed on avionic equipment before the spark gaps in the protecting lightning arrester break down.

Measurements were made of the spectral density of radiation from long electrical arcs used to simulate lightning strokes to aircraft. The relative amplitude at different frequencies seems to agree with that observed from natural lightning, falling at a 1/f rate in the vicinity of 1 MHz.

TABLE OF CONTENTS

TABLES

ILLUSTRATIONS

SECTION 1

1.0 Introduction

This is the second volume of a report covering work done in three broad areas under Contract F33615-70-C-1144/Project 4357, all of the areas dealing with the subject of lightning flashes to aircraft. These three broad areas were:

A) To investigate the direct burning and blasting effects of lightning, particularly as to how they relate to the newer composite panels and structural elements.

B) To investigate the indirect effects of lightning on aircraft, particularly the electromagnetic effects, but also including the physical shock wave from a lightning discharge.

C) To provide investigator services for such special problems as might arise during the course of the contract.

The first volume titled:

"Lightning Effects Relating to Aircraft
Part I - Lightning Effects on and Electromagnetic
Shielding Properties of Boron and Graphite
Reinforced Composite Materials"

covered the effects of lightning discharges on boron-epoxy and graphite- epoxy composite materials and the electromagnetic shielding properties of such materials. The composite materials have many virtues but resistance to the effects of lightning is not one of them. In contrast to aluminum which, by blasting effects of lightning and provides excellent electromagnetic shielding, the composite materials are neither good conductors nor good insulators nor very good in providing shielding against electromagnetic radiation. If these composite materials are used in aircraft in locations where they might be struck by lightning, they will require some form of protection. Questions immediately arise as to how vulnerable are the composite materials to lightning and how best may protection be provided.

This volume deals with the properties of simulated lightning rather than with the properties of materials. In section 2 it covers the effects of simulated lightning strokes on lightning arresters and avionic equipment. A lightning stroke is not an instantaneous phenomena and this work deals with conditions during the preliminary stages of an approaching lightning flash. During the work

the electric fields at the surface of a simulated aircraft were investigated. It was found that streamers from protruding objects on an aircraft tended to limit the electric field strength at the aircraft surface to values of about 100 kilovolts per meter. This figure, coupled with the data on shielding effectiveness of composite materials presented in the companion Part I of this report helps define the internal electromagnetic field environment to which avionic equipment might be exposed.

Section 3 of this report deals with the electrical characteristics of simulated lightning flashes, particularly with the frequency spectrum of radiation from a four meter arc.

Section 6 of this report deals with blast pressure measurements near electrical arcs.

Section 7 of this report deals with services rendered to investigate lightning accidents or lightning incidents to aircraft. A modest amount of time was spent on such activities during the performance of the contract.

SECTION 2

2.0 Effects of Simulated Lightning Strokes on Lightning Arresters and Avionic Equipment

2.1 Introduction

The application of lightning arresters involves two primary considerations: the degree to which the arrester can carry the lightning current to which it is subjected and the degree to which it allows surge voltages to appear on the equipment it is protecting before it switches into its low impedance protecting state. This particular investigation is concerned with this latter problem. In particular it is concerned with the phenomena that occur in and around the aircraft and arrester as a lightning discharge is developing and approaching an aircraft. The electric field in the vicinity of the aircraft reaches very high values during the formative stage of a lightning discharge. This high electric field will cause local discharges from the protruding parts of the aircraft. On electrical elements such as antennas, the discharge current will be conducted into the communication equipment, transmitters and receivers and develop high and possibly dangerous surge voltages before the lightning arrester operates and diverts the current through a supposedly harmless path. The voltages that are produced by these currents are determined by the magnitude of the currents and by the nature of the circuit through which they flow.

A point of terminology should be established here. Typically the currents under concern here are referred to in the literature as predischarge currents and have values typically of 1 - 100 amperes. They are thus distinguished from the high currents, 1000 - 100,000 amperes, that flow when the lightning discharge becomes fully developed.

As a rough rule of thumb the present specification on aircraft lightning arresters (MIL-A-9094 D, March 17, 1969) is concerned with the response of the arrester to final or fully developed lightning discharges. It is not primarily concerned with what happens during the predischarge phase. Possibly consideration of what happens during the predischarge phase should be the concern of those who design the equipment to be protected by the arrester. This thought will be explored in the section on conclusions.

2.2 Tests Performed

The tests were performed using a high voltage impulse generator to simulate the natural stroke and discharging this through a long arc to a short antenna to which an aircraft lightning arrester was connected.

The arresters under test were mounted on an aluminum box as indicated in Figure 1. In the upper part of the box, two similar lightning arresters (L.A.) were placed: in position 1, an L.A. with a porcelain housing and in position 2, an L.A. with a glass housing. These arresters were supplied courtesy of the Dale Electronics Corporation and were respectively a Model LA-13-1 and a Model LA-13-6A. The model LA-13-1 (LA 2) is built to Collins specification 13-1858-030 while the Model LA-13-6A (LA 1) is built to Boeing specification D10-2701-1. They have been used on the B-58G (LA 2) and on the KC-135 (LA 1).

The 4' x 4' x 8' aluminum box was left over from an earlier and unrelated contract. It was used primarily because it provided good electromagnetic shielding for the dummy circuits upon which voltage was to be measured and because it simulated in a crude sense an aircraft fuselage.

Atop each of the arresters was mounted a short (1 ft.) electrode of 0.5" square brass rod. This was to duplicate a short aircraft antenna from which a predischarge current could be drawn. In position 3 on the box there was mounted another electrode projecting the same height above the box as those electrodes mounted on the arresters. This electrode was mounted on a feed-through insulator and connected inside the box to a current shunt. In the fourth position there was mounted an electric field probe that recorded the electric field strength near the electrodes on the arresters. The electric field strength so measured is comparable to what would be measured on a smooth portion of an aircraft as a lightning discharge was developing and approaching the aircraft.

Above the box was positioned a rod type high voltage electrode. This electrode could be positioned above any of the three lower electrodes. The spacing of the gap between the upper and lower electrodes was 0.75 meters, the maximum distance that could be consistently flashed over by the 500 kV impulse generator used to initiate the discharges.

The following measurements were taken:

1. The magnitude and the rate of change of the voltage applied to the gap between the arcing electrode and the grounded enclosure. This could be viewed as the voltage between the aircraft and an approaching lightning discharge. This voltage was measured by a resistive impulse voltage divider connected between the high voltage electrode and the grounded aluminum case. The output of this divider was displayed on a recording oscilloscope, Tektronix Type 507.

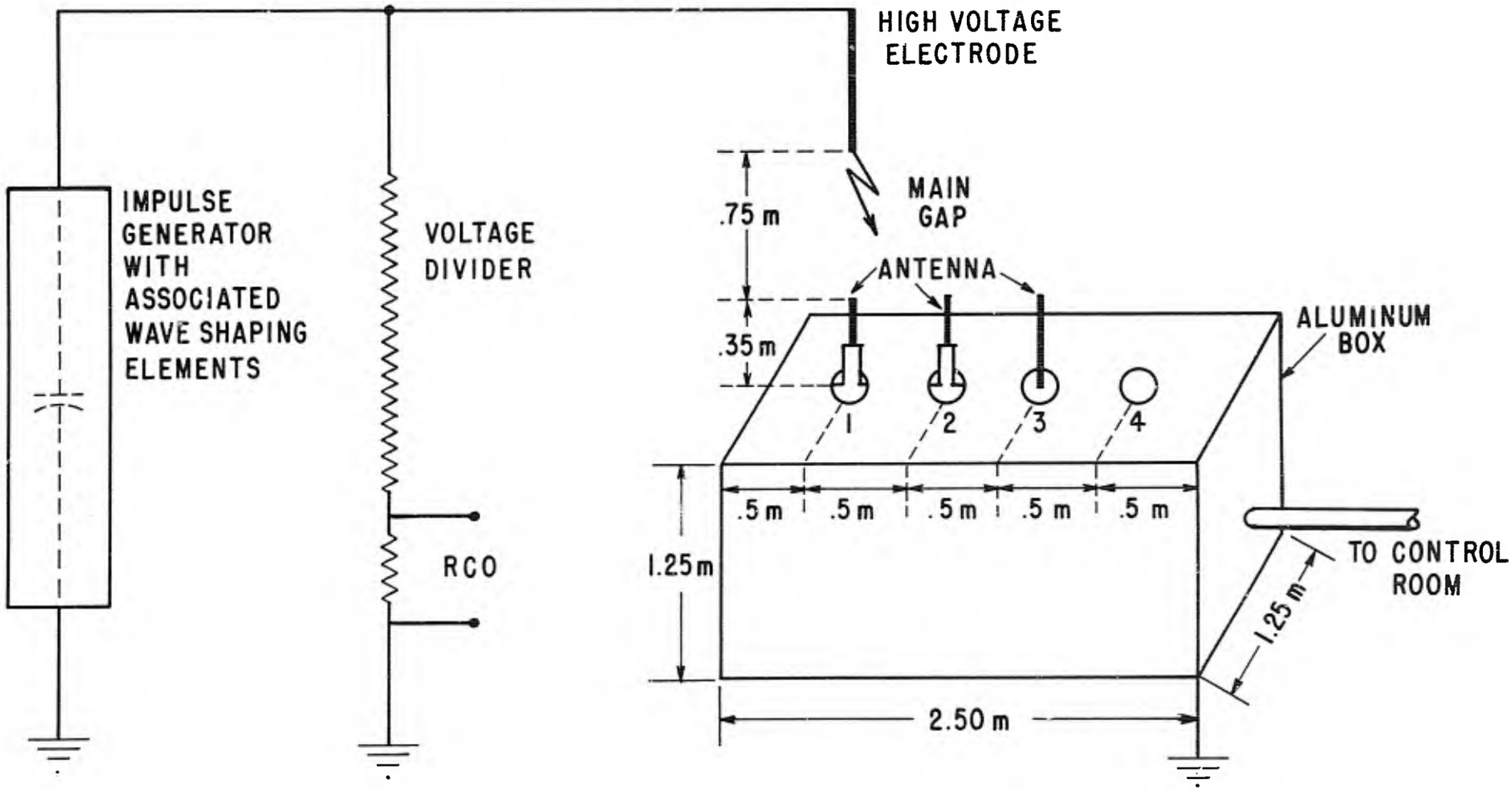

FIGURE 1

General Arrangement of Test Circuit

2. The rate of rise and the magnitude of the voltage applied to the simulated avionic equipment connected to the antenna. This was measured by 10.3 kΩ voltage dividers connected between the output of the arrester and ground. One divider was used on each arrester. The dividers were placed inside the aluminum box and were further shielded against interfering electrical signals by a metallic shield placed around the divider and the lower end of the arrester. Two different load circuits were simulated, as indicated on Figure 2. First, a high impedance resistor of 10.3 kΩ only was used and then a tuned circuit, having the high impedance resistor in parallel. The tuned circuit had a 100 pF capacitor and a 13.4 μH inductor in parallel. The oscillatory frequency of the tuned circuit was thus 4.3 MHz. The 10.3 kΩ resistor was in fact the voltage divider. This could basically be considered an open circuit in comparison to the normal surge impedance of any cable connecting the arrester to a transmitter or receiver.

3. The magnitude and rate of rise of the stroke current. This measurement was mainly performed on a 10.1Ω shunt connected to the antenna in position 3 to evaluate the total charge that was coming into the antenna connected to the L.A. in the testing conditions. Tests were also carried out placing the shunt electrically between the external flange of the L.A. and the grounded box to evaluate the charges that were going to ground through the L.A. internal gap. The test connections in the first condition are indicated in Figure 2. A spark gap connected across the shunt limited the voltage applied to the recording oscilloscope when a breakdown occurred between the high and low voltage electrodes.

4. The total charge transferred to the lower rod of the main gap. This evaluation was done graphically from the oscillographic measurement of the current versus time to reduce the number of simultaneous oscillographic measurements taken during the test. However, the total charge transferred during these tests does not represent the total charge transferred in an actual lightning stroke since the bulk of the natural stroke is transferred by the continuing currents between the individual high current lightning strokes. It represents only the charge transferred during the predischarge phase.

5. The magnitude and the rate of rise of the electric field at different distances from the higher rod. This measurement was done with the technique suggested from Meek & Collins.[1] It involves the measurement of the charge induced on a small probe mounted flush with the surface of the box. A changing electric field external to the box will induce a displacement

1. S.M. Meek, M.M.C. Collins, "Measurement of Electric Fields at Electrode Surfaces". Electronics Letters - June 1965 - Volume 1, #4, pp. 110-111.

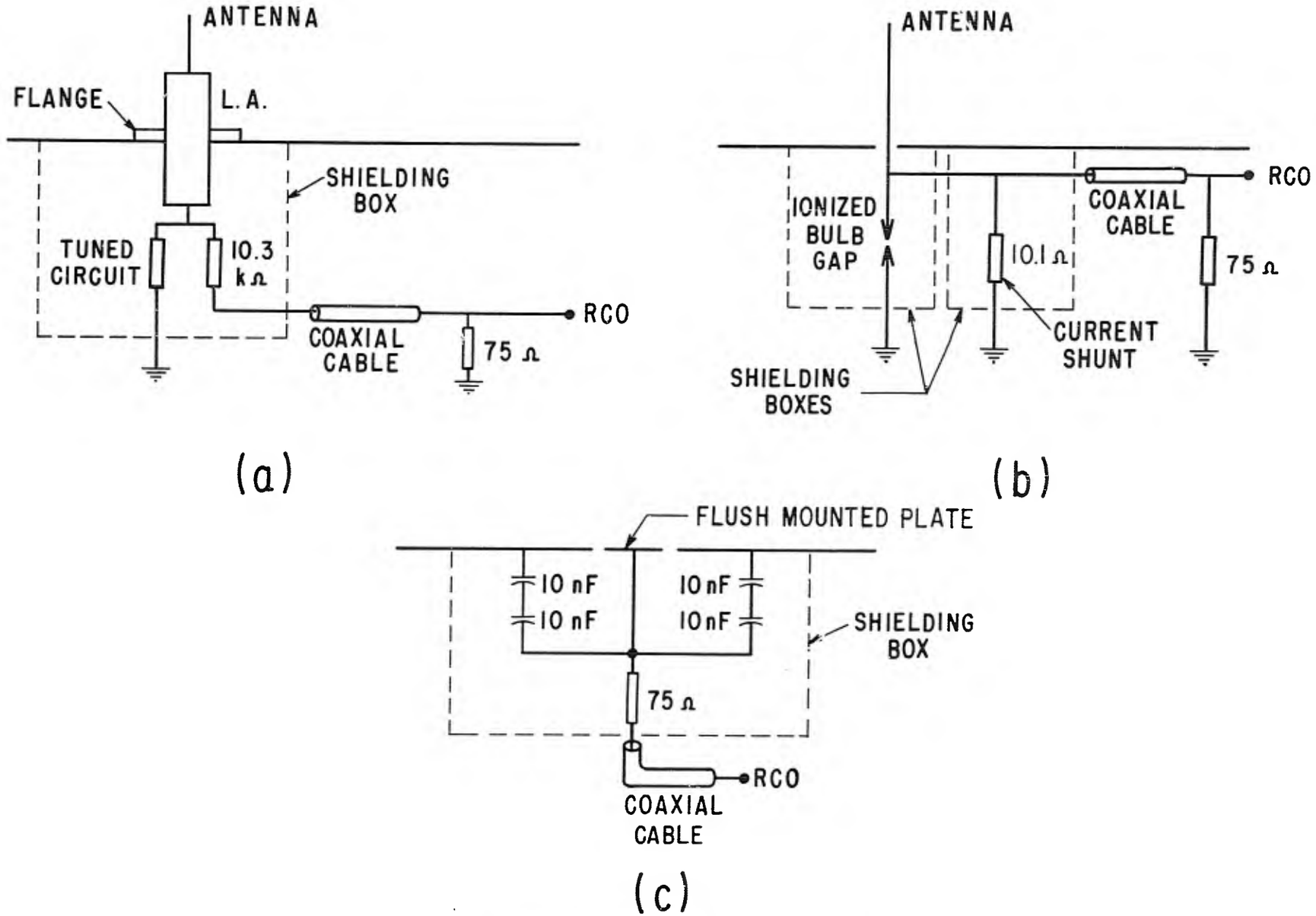

FIGURE 2 - Test Circuit Arrangements for Measuring
(a) Voltage Across Avionics Equipment
(b) Current Through Lower Rod
(c) Electric Field on Plant

current onto the collector plate of magnitude proportional to the area of the plate and the time rate of change of the electric field. If this current is integrated in a capacitor, the voltage developed across this capacitor is then proportional to the external electric field strength. The governing relationships would then be

$$V(t) = \frac{1}{C} \int A \frac{dD}{dt} = \frac{A\epsilon_o}{C} E(t)$$

where $V(t)$ = output voltage from the probe

A = surface area of the collector plate

D = displacement current per unit area

ϵ = absolute permittivity

C = value of the integrating capacitor

$E(t)$ = electric field strength

The calibration of the circuit was done by placing a plate at a known distance from the probe and applying a square wave voltage between this and the ground. The probe surface was of 33cm^2 and not smaller because we were concerned with the average field near the arresters. It might be noted that others have used probes of a similar type in the end of an electrode to record the electric field strength directly in the gap. All the shielded measurement circuits were placed inside the box and the coaxial cables were taken to the control room through a shielded conduit. The shielding was sufficient that there were no problems with spurious electric signals induced onto the measurement leads by the high voltage circuits. Figure 3 shows the electric field measurements configuration.

2.3 Test Results

2.3.1 Measurement of the Voltage Applied to the Avionic Equipment

2.3.1.1 Load with a High Impedance Resistor

Tests were carried out with surges of both positive polarity and negative polarity applied to the high voltage electrode. When testing with positive polarity a voltage of 395 kV could be applied before complete breakdown of gap occurred. With negative polarity a higher voltage, 510 kV, could be applied before breakdown occurred. These correspond to average gradients across the gap of 5.3 kV/cm for positive polarity and 6.8 kV/cm for negative polarity.

No fundamental difference was noted in the basic performance of the two arresters and the considerations that can be deduced are the same for each of them. The results obtained with the arresters in position 1 & 2 are respectively indicated on Tables I and II; the type of oscillograms obtained are indicated in Figure 3 and Figure 4 for the negative and positive polarity respectively.

When an impulse of negative polarity is applied to the main gap, an impulse as on Figure 3a appears across the load. The duration of this impulse is about 2 μs and it remains roughly the same at all the voltage levels. The amplitude increases however with the applied voltage from 1.4 kV for an applied voltage of 240 kV up to 4.0 kV for an applied voltage of 520 kV. This pulse appears to be due to the capacitive charging current drawn across the gap by the changing electric field.

When the applied voltage was increased, a second impulse appeared (Figure 3b. For the L.A. in position 1 it was first noted at the voltage level of 380 kV, for the other in position 2, it was seen at 310 kV. The duration of this impulse is about 1 μs and when it first appears it starts 6 - 10 μs after the beginning of the first one. For L.A. 1 only, some other small peaks were noted after the second one (Figure 3c). As the applied voltage was increased, the second impulse also increased in amplitude and occurred at earlier times. The successive small predischarges did not increase and eventually became negligible in amplitude. With higher applied voltages, the second impulse occurs early enough to be superimposed on the first impulse (Figure 3e. . When the applied voltage is increased still more, a flashover occurs and the voltage across the avionic equipment has the shape as indicated in Figure 3f. The maximum peak of the voltage occurs before the flashover of the main gap and its value reaches about 15 kV for L.A. 1 and 31 kV for L.A. 2.

TABLE I

Voltage Across the Resistive Load for the Lightning Arrester #1

Negative Polarity					Positive Polarity				
Applied Voltage (kV)	First Peak of Voltage (kV)	Second Peak of Voltage (kV)	Maximum Peak of Voltage (kV)	Refer to Figure	Applied Voltage (kV)	First Peak of Voltage (kV)	Second Peak of Voltage (kV)	Maximum Peak of Voltage (kV)	Refer to Figure
236	1.4			3a	158	1.1			4a
268	1.7			3a	193	1.4			4a
308	2.0			3a	232	1.8			4a
344	2.4			3a	272	2.1			4a
384	2.6	0-4		3a,3b,3c	308	2.6			4a
422	2.7	2-5		3b,3c	345	3.0			4a
456	3.3	7-10		3b	378	3.6	2		4b,4c
473	3.9	7	11-15	3b,3f	390	3.7	3-5		4b,4c
486	3.9	6	11-15	3b,3f	398	3.7	7-9	20-27	4c,4d
515	3.9	6	11-15	3b,3f	403	3.8	7-9	20-27	4d
520	3.9	6-12	9-13	3f	420	4.6	10	17-29	4d
547			10-11	3f	454	4.6		25-28	4d

TABLE II

Voltage Across the Resistive Load for the Lightning Arrester #2

Negative Polarity					Positive Polarity				
Applied Voltage (kV)	First Peak of Voltage (kV)	Second Peak of Voltage (kV)	Maximum Peak of Voltage (kV)	Refer to Figure	Applied Voltage (kV)	First Peak of Voltage (kV)	Second Peak of Voltage (kV)	Maximum Peak of Voltage (kV)	Refer to Figure
233	1.3			3a	159	1			4a
272	1.5			3a	192	1.2			4a
308	1.8	1.3		3b	233	1.5			4a
344	2.0	2.5		3b	270	1.9			4a
387	2.2	3.5		3d	307	2.3			4a
422	2.8	4.3		3d	346	2.7			4a
455	2.8	5.1		3d,3e	382	2.9	1-2		4c
486	3.0	7		3e	390	3.0	3		4c
497	3.0	6		3e	396	3.3	4		4c
521	3.2	6.5	27-31	3e,3f	400		4-6	23	4c,4d
545			30-31	3f	414			23	4d
560			30-31	3f	454			23	4d

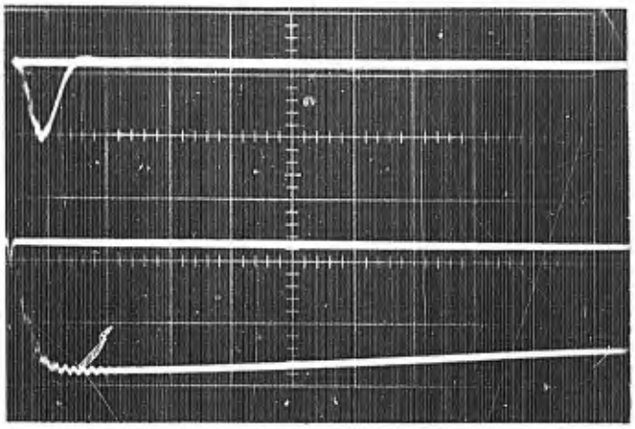

(a) Upper 1.38 kV/div. 2 μs/div.
Lower 0.3 kV/cm/div. 2 μs/div.

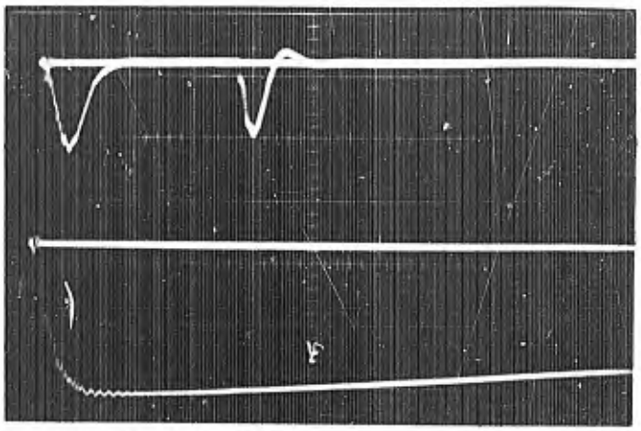

(b) Upper 1.38 kV/div. 2 μs/div.
Lower 0.3 kV/cm/div. 2 μs/div.

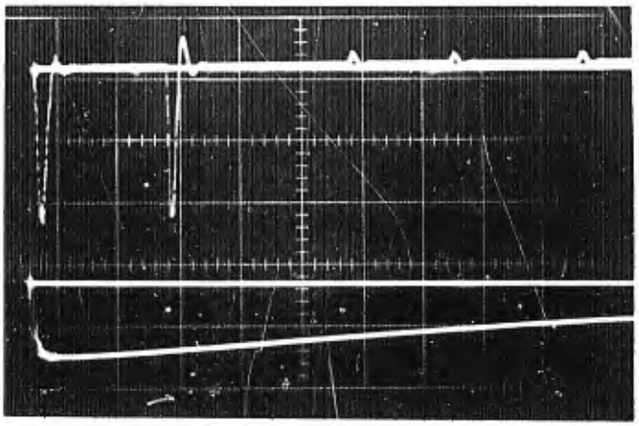

(c) Upper 0.69 kV/div. 5 μs/div.
Lower 0.6 kV/cm/div. 5 μs/div.

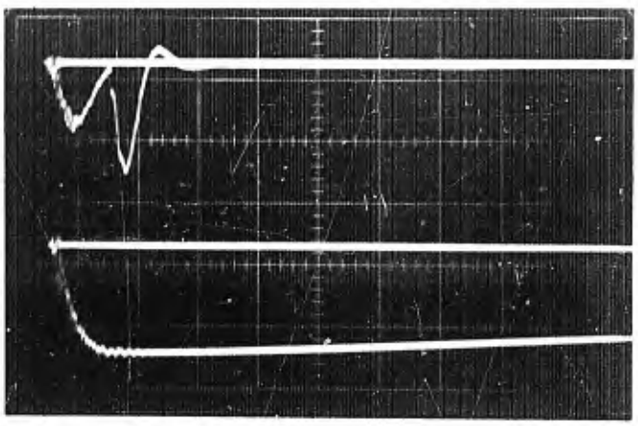

(d) Upper 2.76 kV/div. 2 μs/div.
Lower 0.6 kV/cm/div. 2 μs/div.

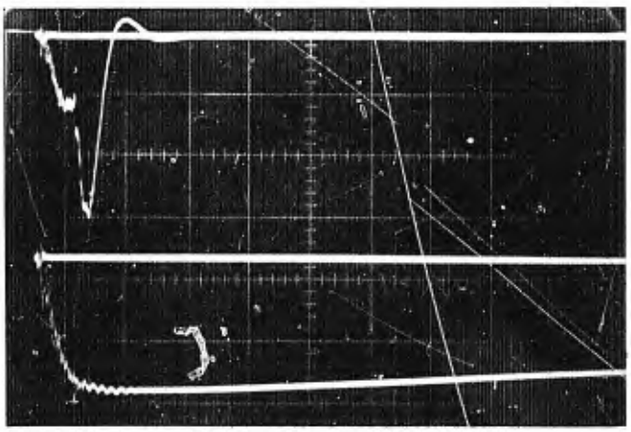

(e) Upper 2.75 kV/div. 2 μs/div.
Lower 0.6 kV/cm/div. 2 μs/div.

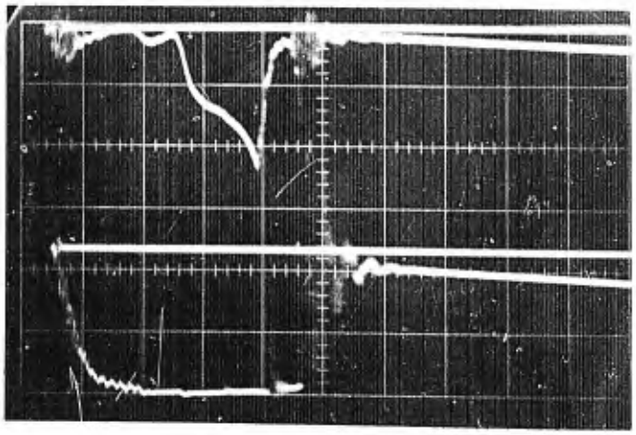

(f) Upper 16.6 kV/div. 2 μs/div.
Lower 0.6 kV/cm/div. 2 μs/div.

Upper Traces - Voltage Applied to Resistive Load
Lower Traces - Electric Field

FIGURE 3 - Effects with Resistive Load - Negative Polarity

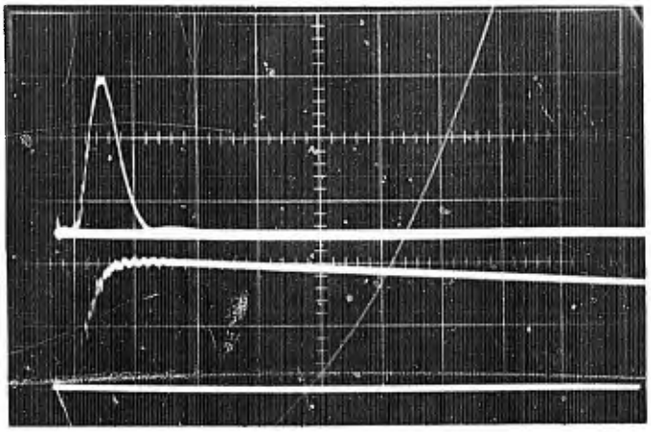

(a) Upper 0.69 kV/div. 2 μs/div.
Lower 0.3 kV/cm/div. 2 μs/div.

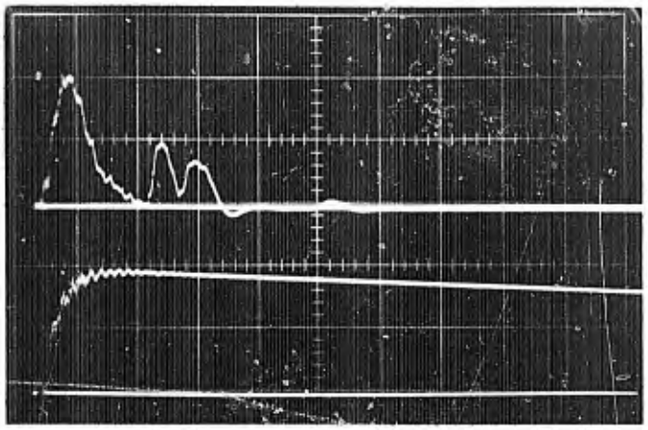

(b) Upper 1.38 kV/div. 2 μs/div.
Lower 0.6 kV/cm/div. 2 μs/div.

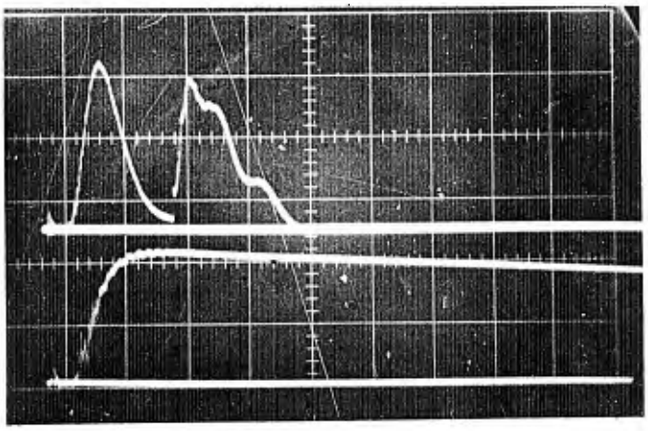

(c) Upper 1.38 kV/div. 2 μs/div.
Lower 0.6 kV/cm/div. 2 μs/div.

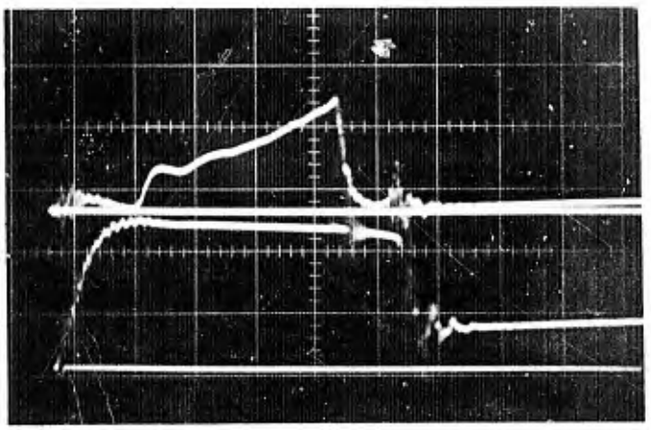

(d) Upper 16.6 kV/div. 2 μs/div.
Lower 0.6 kV/cm/div. 2 μs/div.

Upper Traces - Voltage Applied to Resistive Load
Lower Traces - Electric Field

FIGURE 4 - Effects With Resistive Load - Positive Polarity

Presumably the current in the high voltage gap begins to increase in an avalanche mode until the voltage drop across the 10.3 kΩ resistance voltage divider becomes high enough to cause the surge-diverting gap of the lightning arrester to fire. This corresponds to a predischarge current of 1.45 amperes for LA 1 and 3.0 amperes for LA 2.

When an impulse of positive polarity is applied to the main gap, similar phenomena occur. At the lower applied voltages as indicated on Figure 4a. an impulse appears across the avionic equipment. The duration of this impulse is again approximately 2 μs and its amplitude increases with the applied voltage, increasing from 1 kV for an applied voltage of 150 kV to 5 - 6 kV for an applied voltage of 450 kV. At an applied voltage of about 380 kV a second impulse appears with waveshape as on Figure 4b or 4c. The length of this impulse is about 4 μs and its amplitude can reach 10 kV. When a flashover in the main gap occurs, the voltage across the avionic equipment assumes a shape similar to that with negative polarity as indicated on Figure 4d. The maximum peak of the voltage that was reached was 25 - 28 kV for LA 1 and 23 kV for LA 2. These correspond to currents of 2.2 - 2.7 amperes. Again these currents develop sufficient voltage across the 10.3 kΩ resistive load to cause a breakdown of the surge diverting gaps of the arrester.

The most significant point to observe here is that voltage surges of several microseconds duration can be passed by an arrester during the predischarge stage of a developing breakdown and that these voltages (or the predischarge currents that cause the voltages) can lead to breakdown of the lightning arrester well before any high current discharge begins to flow in the high voltage region external to the lightning arrester.

2.3.1.2 Load with a Tuned Circuit

Tests were carried out on both arresters with both polarities of applied voltage. The type of oscillograms obtained are indicated on Figures 115 and 116 for the negative and positive polarity respectively. Again no fundamental difference was noted in the performance of both the arresters.

When a voltage of negative polarity is applied to the main gap, an impulse as indicated on Figure 5a appears across the load circuit. The peak of this oscillating impulse increases with the applied voltage but the values are much lower than measured with the 10.3 kΩ resistance load. The maximum was about 300 - 400 volts. A second oscillating impulse (Figure 5b appears at the same

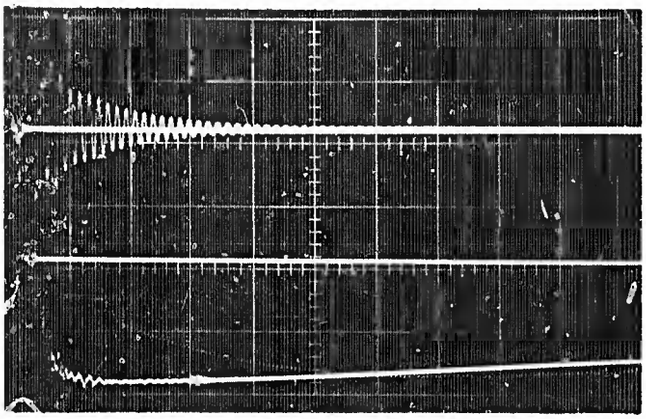

(a) Upper 67.5 V/div. 2 μs/div.
Lower 0.3 kV/cm/div. 2 μs/div.

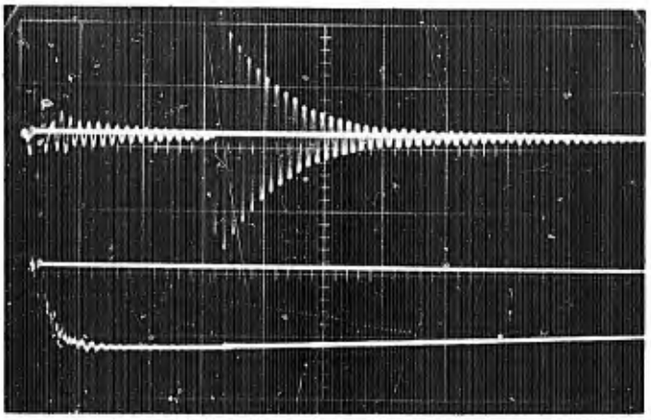

(b) Upper 266 V/div. 2 μs/div.
Lower 0.6 kV/cm/div. 2 μs/div.

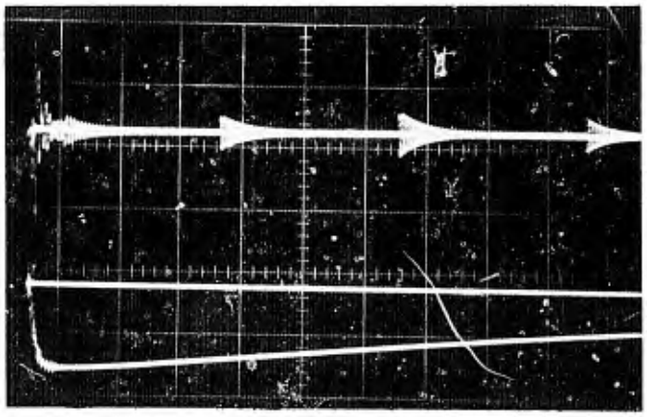

(c) Upper 13.3 V/div. 5 μs/div.
Lower 0.6 kV/cm/div. 5 μs/div.

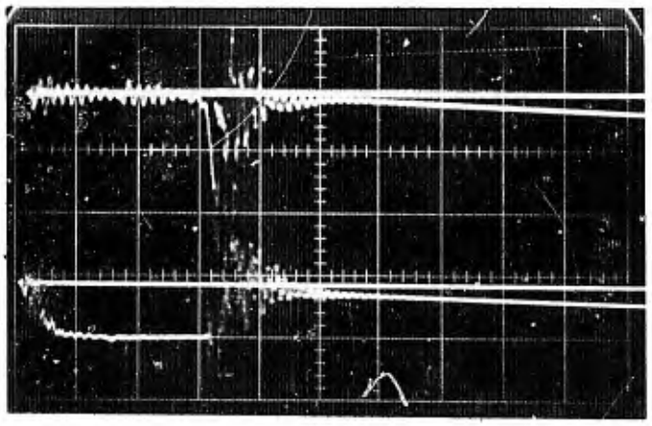

(d) Upper 5.32 kV/div. 2 μs/div.
Lower 1.5 kV/cm/div. 2 μs/div.

Upper Traces - Voltage Applied to Tuned Load
Lower Traces - Electric Field

FIGURE 5 - Effects With Tuned Load of Avionics Equipment - Negative Polarity

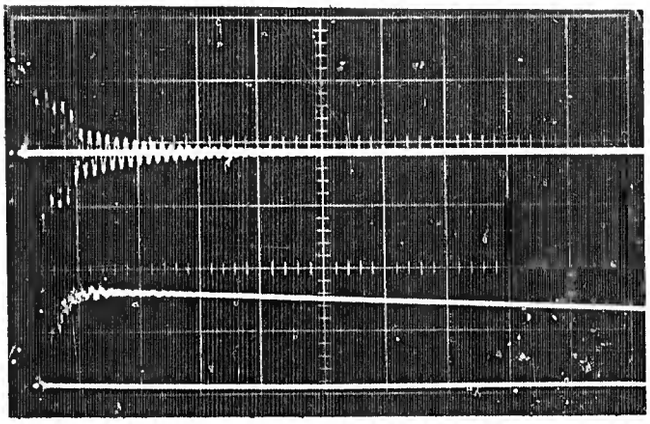

(a) Upper 67.5 V/div. 2 μs/div.
Lower 0.3 kV/cm/div. 2 μs/div.

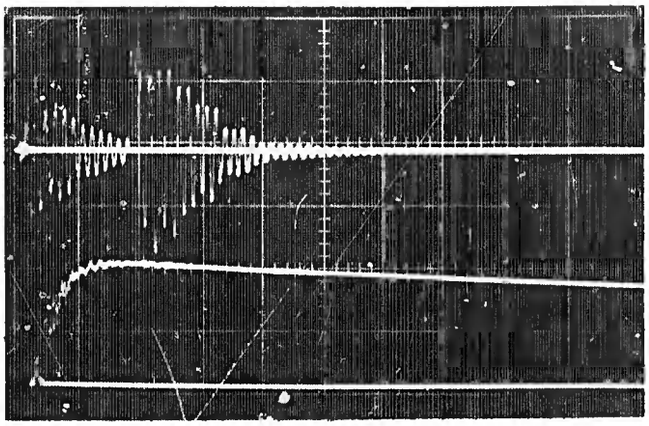

(b) Upper 133 V/div. 2 μs/div.
Lower 0.6 kV/cm/div. 2 μs/div.

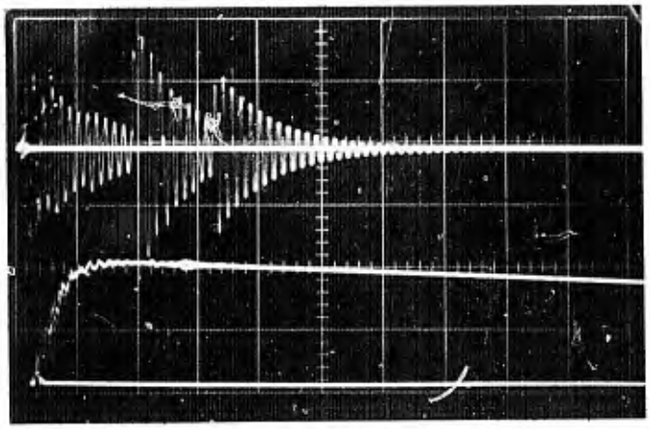

(c) Upper 133 V/div. 2 μs/div.
Lower 0.6 kV/cm/div. 2 μs/div.

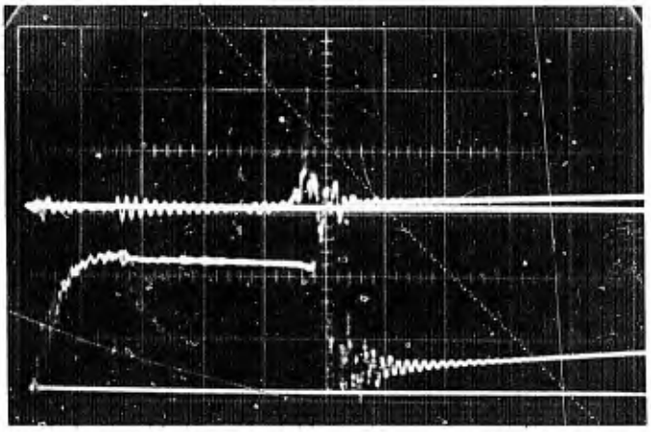

(d) Upper 5.32 kV/div. 2 μs/div.
Lower 0.6 kV/cm/div. 2 μs/div.

Upper Traces - Voltage Applied to Tuned Load
Lower Traces - Electric Field

FIGURE 6 - Effects With Tuned Load of Avionics Equipment - Positive Polarity

voltage levels and with the same characteristics as before but the maximum peak value that can be reached now is about 1 kV. Also here many peaks were noticed after the second one (Figure 5c) with the LA 1, but their amplitude does not increase with higher voltages. Finally, when the applied voltage is high enough to spark the main gap, the voltage across the avionic equipment has the shape indicated on Figure 5d and the maximum peak value reaches 9 - 10 kV.

When a voltage of positive polarity is applied to the main gap, an impulse as indicated on Figure 6a appears. The peak amplitude increases with the applied voltage but the maximum does not go over 200 volts. Increasing the applied voltage leads to a second and sometimes a third impulse appears as on Figure 6b and 6c. The maximum amplitude can reach 500 volts. When a flashover occurs on the main gap, the shape of the voltage across the load is as on Figure 6d and the maximum peak value is 10 - 11 kV.

2.3.2 Measurement of Stroke and Predischarge Currents

The voltages measured in the previous section were caused by the current flowing through the 10.3 kΩ resistor in one case or by the current pulses shock-exciting a tuned circuit in the other case. In either case the voltage depends on the amplitude and duration of the current pulses. These are primarily determined by the physical characteristics of the antenna connected to the arrester and by the strength and time behavior of the external electric field. They are in part, however, determined by characteristics of the avionic load through which the currents must flow. The measurements made with the 10.3 kΩ resistor represented basically a measurement of the open circuit voltage. Measurements were also made of the current that would flow under conditions where (presumably) the current was controlled only by conditions in the high voltage field and not by the impedance of the load to which the arrester is connected.

The stroke current was measured having the antenna grounded directly through the measurement shunt. As mentioned earlier this shunt had a resistance of 10 ohms. This was not sufficient to have a limiting effect on the predischarge currents.

A summary of test results is indicated on Table III.

With negative polarity, a peak of current with many high frequency oscillations was measured (Figure 7a). The duration of this peak was about 1.2 μs. Its amplitude increased with the applied voltage reaching a maximum peak value

TABLE III

Prebreakdown Current of the Main Gap Without Lightning Arrester

Negative Polarity					Positive Polarity				
Applied Voltage (kV)	First Peak of Current (A)	Second Peak of Current (A)	Max. Peak of Current before Flashover (A)	Refer to Figure	Applied Voltage (kV)	First Peak of Current (A)	Second Peak of Current (A)	Max. Peak of Current before Flashover (A)	Refer to Figure
235	.36			7a	194	.7			8a
272	.4			7a	232	.96			8a
308	1.1			7a	268	1.0			8a
342	1.1			7a	309	1.0			8a
381	1.1	2.2		7b	346	1.0			8a
417	1.2	3.5		7b	376	1.0	1-1.6		8b
455	1.2	3-6.6		7b	389	1.0	1.2-2.6	24-27	8b,8c
502	1.2		70-90	7b,7c	392	1.0	1.8-3.0	24-27	8b,8c
512	1.2		70-90	7b,7c	398	1.0	3-4	24-27	8b,8c

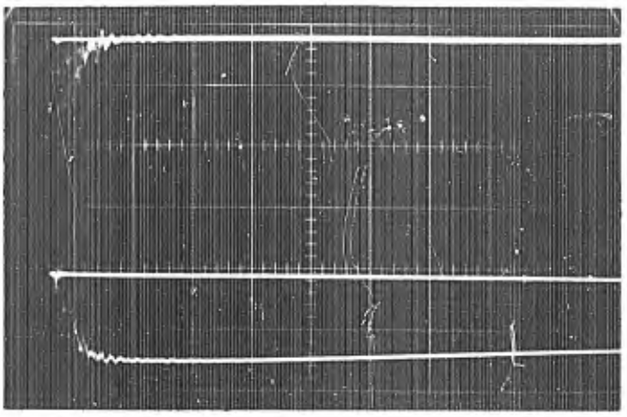

(a) Upper 0.5 A/div. 2 μs/div.
Lower 0.6 kV/cm/div. 2 μs/div.

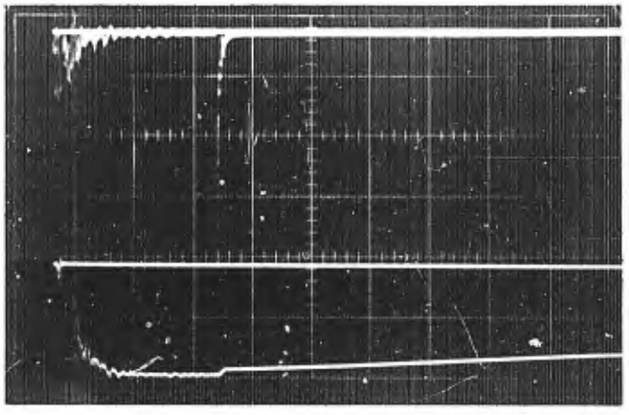

(b) Upper 0.5 A/div. 2 μs/div.
Lower 0.6 kV/cm/div. 2 μs/div.

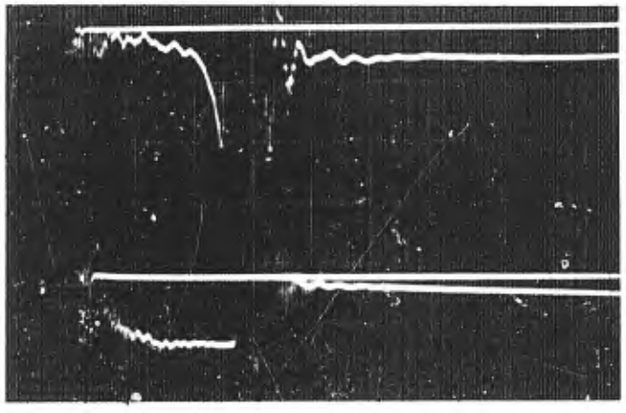

(c) Upper 36 A/div. 2 μs/div.
Lower 1.5 kV/cm/div. 2 μs/div.

Upper Traces - Prebreakdown Current
Lower Traces - Electric Field

FIGURE 7 - Prebreakdown Current and Electric Field Without Lightning Arresters - Negative Polarity

19

of about 1.2 A at 500 kV. At 350 kV a second current pulse appeared (Figure 7b). This was of very short duration. As the applied voltage was increased, this current pulse grew larger and occurred at earlier times, just as did the voltage pulses observed on the 10.3 k_{Ω} load. This current pulse reached values of 6.6 amperes before the flashover of the main gap occurred.

At voltages of about 500 kV a flashover of the main gap can occur and the waveshape of the current assumes the configuration of Figure 7c. In this case many small peaks can be noted. These currents grow as an avalanche reaching values of 70 - 90A before the spark gap across the shunt sparks to ground.

With a positive polarity applied voltage the phenomena is virtually identical.

A first peak with high frequency oscillations appears in the beginning (Figure 8a). Its duration is about 1.2 μs and the maximum of its amplitude is about 1A. As the applied voltage is increased other peaks follow the first one (Figure 8b) and their amplitude is larger, reaching values of 4 amperes. At 390 kV a flashover can occur and, in this case, the shape of the current is roughly the same as that seen on the negative polarity (Figure 8c). The maximum peak can reach about 25 A.before the protective spark gap on the current shunt flashes over and removes the signal. On positive polarity, as on negative polarity, the protective gap flashes over before the air gap between the high and low voltage electrodes breaks down.

Some current measurements were also taken on the lightning arrester 2. During withstand tests (Figure 9) the peak values were generally smaller than those obtained earlier; during flashover tests the shape was always similar to that measured with the shunt. In both the cases, however, a less linear trace was noted due to the necessity to spark also the internal lightning arrester gap.

2.3.3 Electric Field Measurement

The field at position 4 was measured every time, whether the upper rod was above LA 1 (position 1), LA 2 (position 2) or over the current shunt (position 3). From all the oscillograms, as indicated on Figures 3 through 9, it can be seen that the waveshape of the field is almost the same as the applied voltage. The waveshape of the electric field at the surface of the box however should not in general be the same as the waveshape of the voltage applied to the high voltage electrode. In the absence of any electrical discharge from either the upper or lower electrode, the field at the surface of the box will be the same

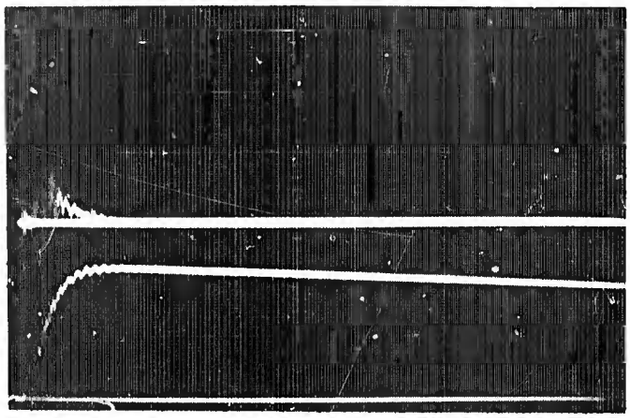

(a) Upper 0.4 A/div. 2 μs/div.
Lower 0.6 kV/cm/div. 2 μs/div.

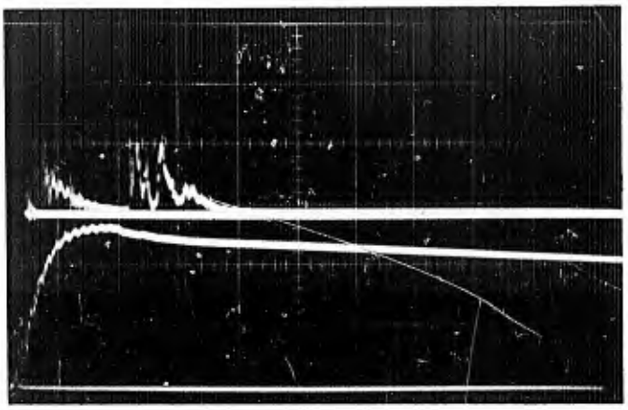

(b) Upper 0.4 A/div. 2 μs/div.
Lower 0.6 kV/cm/div. 2 μs/div.

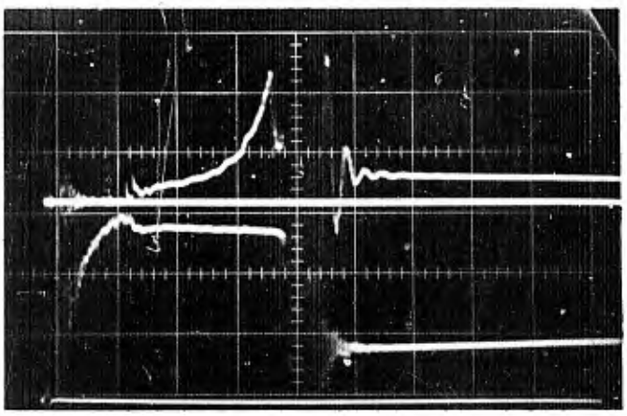

(c) Upper 12 A/div. . 2 μs div.
Lower 0.6 kV/cm/div. 2 μs/div.

Upper Traces - Prebreakdown Current
Lower Traces - Electric Field

FIGURE 8 - Prebreakdown Current and Electric Field Without Lightning Arresters - Positive Polarity

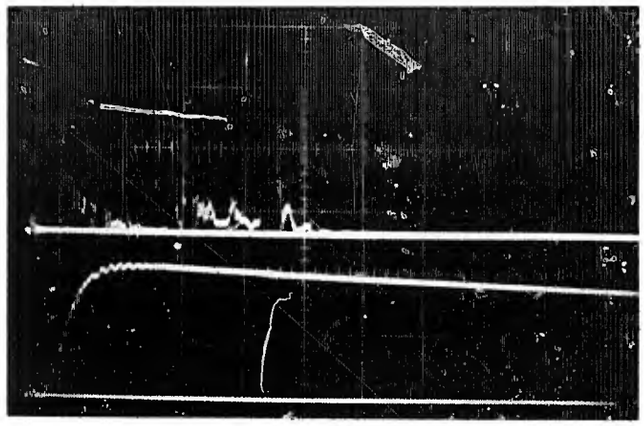

Upper Trace - Prebreakdown Current	0.2 A/div. 2 μs/div.
Lower Trace - Electric Field	0.6 kV/cm/div. 2 μs/div.

FIGURE 9 - Prebreakdown Current and Electric Field with Lightning Arresters - Positive Polarity

shape as the voltage applied to the electrodes. The field intensity will be proportional to the geometry of the electrodes and can be determined, in principle at least, analytically from a mathematical description of the geometry. This field intensity would be directly proportional to the applied voltage. Because it is determined only from geometrical considerations, it is sometimes referred to as the geometrical field.

When ionization takes place the actual field strength may be either greater or less than the geometrical field. If a streamer develops from the high voltage electrode and propagates toward the ground, the upper electrode is in effect moved closer to the surface of the box. Such a streamer would act to increase the actual field at the surface of the box and make it larger than the equivalent geometrical field. If a streamer develops from the lower electrode and moves upward, it in effect extends the grounded electrode and partially shields the adjacent surfaces of the box from the upper electrode. In such a case the actual electric field strength at the surface of the box would be less than the geometric field strength. Examples of this latter effect can be seen on the oscillograms of Figures 7b, 7c, 8b and 8c. Since the electric field strength decreased when the predischarge current pulse occurred, the conclusion would be that a streamer has developed from the lower electrode. This effect only shows up when the upper electrode was positioned over the electrode closest to the electric field sensing plate. Presumably the same effect occurs on the surface of the box next to the other electrodes, but the electrodes are too far away to have any effect on the electric field at the one point on the box that was instrumented.

The actual electric field can be greatly different than the geometric field, depending on where one measures the field. In order to see how the actual field was influenced in this particular case, we ran a series of tests comparing the actual field to the applied test voltage. The measured values for three different distances and for both the polarities are plotted on Figure 10 versus the applied voltage.

Obviously the field increases with the applied voltage, for both the polarities, and it decreases with the distance from the point where the arc took place.

The shape of the curves is significant. The first point worthy of note is that in all cases the actual field increases faster than the applied voltage. This is an indication that the space charge at the upper electrode, which increases the actual field, is more intense than the space charge around the

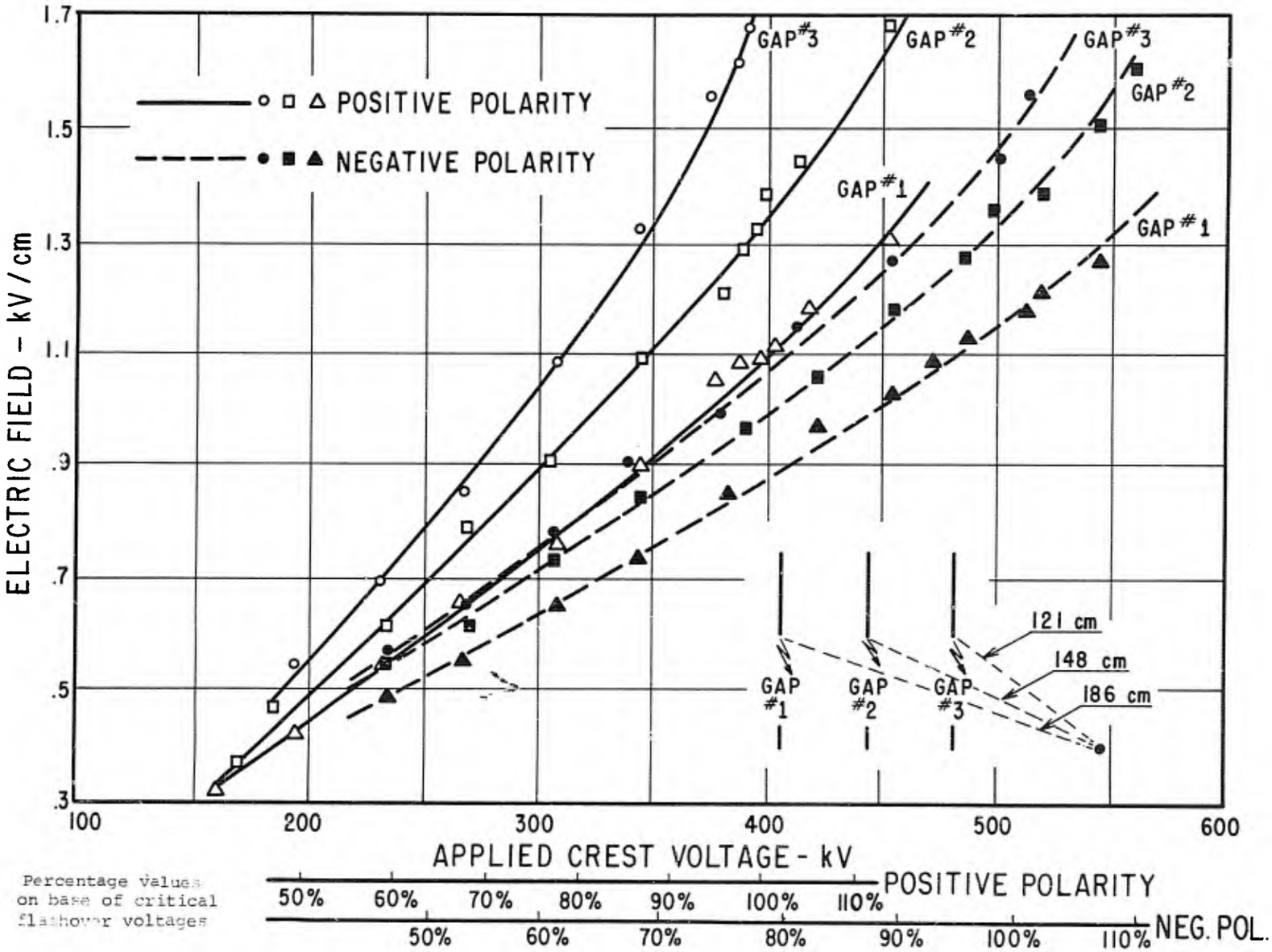

FIGURE 10 - Measured Electric Field Versus Applied Crest Voltage for Positive and Negative Polarities at Different Distances from Upper Rod

lower electrode. The second point worthy of note is that the actual field is higher for positive polarity than for negative polarity. For example with the upper rod positioned over LA 1 (gap #1) the electric field at 400 kV negative applied voltage is about 870 volts per centimeter while it is 1100 volts per centimeter at 400 kV positive applied voltage.

Included on this figure are scales relating the applied voltage to the voltage required to cause flashover of the gap. Thus a positive voltage of about 400 kV can be considered as the 100% critical flashover voltage while with negative polarity the 100% critical flashover voltage is 510 kV. Voltages greater than 100% of the critical flashover voltage can be applied to the gap; they just lead to flashover at a shorter time. When the actual field strengths for positive and negative polarity are compared on the basis of the percentage of the voltage required to produce a complete breakdown of the gap, a third point of interest becomes evident: that there is in fact little difference between positive and negative polarity. As examples a positive polarity voltage of 100% of the critical breakdown voltage applied to gap #1 causes an actual field of 1110 volts/cm at the location of the sensing plate while a negative voltage of 100% gave a field of 1180 volts/cm.

The fourth point worthy of note is that an electrical breakdown is likely to be occurring from nearby protruding objects when the electric field strength at a flat surface on the box reaches values greater than 800 - 1000 volts/cm.

This data might be compared to some obtained by Messrs. Gallimberti, Rea and Baldo.[2]

These investigators suspended a rod electrode 150 cm over a flat metal ground plane and then applied negative impulse voltages of 1.2 x 50 μs wave-shape. Critical breakdown voltage for this gap was 1360 kV. Critical breakdown voltage is that voltage at which 50% of the impulses applied will cause breakdown. They then measured the current flowing in the high voltage rod to

---

2. Field and Current Measurements During Negative Rod-Plane Discharges in Long Air Gaps (*), I. Gallimberti, M. Rea (**).

   Earthed Rod Influence on the Negative Rod-Rod Gaps Breakdown(*), C. Baldo, M. Rea (**).

   (University of Padova, Italy, Istituto Di Elettrotecnica E Di Elettronica) UPee-69/67, April, 1969.

   (*) Presented at the IX International Conference on Ionization Phenomena in Gases. Bucharest 1969.

   (**) High Voltage Research Group of C.N.R..

which the impulse was applied and measured the electric field strength at the surface of the grounded plane. They did not measure current from protruding objects on the plane. An example of their results is shown in Figure 11. Shown are two sets of oscillograms, one of an impulse that caused breakdown and one at the same voltage that did not cause breakdown.

When the electric field at the surface of the plane reached about 1500 volts/cm, a discharge occurred from the high voltage rod reaching currents of 60 amperes. Current from a protruding rod on the plane, had one been present, would have been less. In our tests, discharges from a protruding rod began to occur when the field on the plane reached levels of 800 - 1000 volts per centimeter at a point somewhat removed from the electrodes. The charge liberated from this electrode then tended to increase the actual field at the surface of the plane. The field increased in jumps as successive smaller discharges took place from the high voltage electrode and lowered charge into the space above the electric field probe. Since there is no definite relationship between the size of the jumps in the increasing field and the current emitted from the rod, the conclusion that can be reached is that charge in the gap was moving closer to the plane. A given charge will have more effect on the field at the plane the closer it gets to the field sensing probe. When breakdown did occur, it involved discharges that were initiated from the plane. The presence of these streamers is indicated by the fact that the electric field strength at the plane decreased.

A brief summary of the work of these investigators is given in Table IV, reproduced from their papers.

TABLE IV

Summary of Field and Current Measurements During Negative Rod-Plane Discharges in 150 cm Air Gaps

Voltage	I_p (A)	T (μs)	Q (μC)	E_g (kV/cm)	E_a (kV/cm)
50% V_s	4-10	1-1.5	5-6	1.5	2
80% V_s	30-50	3-5	20-21	2.4	4-5
90% V_s	40-60	4-6	25-27	2.7	5-7
100% V_s	60-100	5-8	32-34	3	5-10

I_p = Peak value of the predischarge current from the impulsed electrode
T = Time to extinction of the predischarge current
Q = Charge injected into the gap = $\int I\,dt$
E_g = Geometrical field strength at the ground plane
E_a = Actual field strength

3.3.4 Charge Transfer

The total charge transferred to the lower rod was calculated averaging all the current measurements taken at each voltage level for both the polarities.

A. No Breakdown

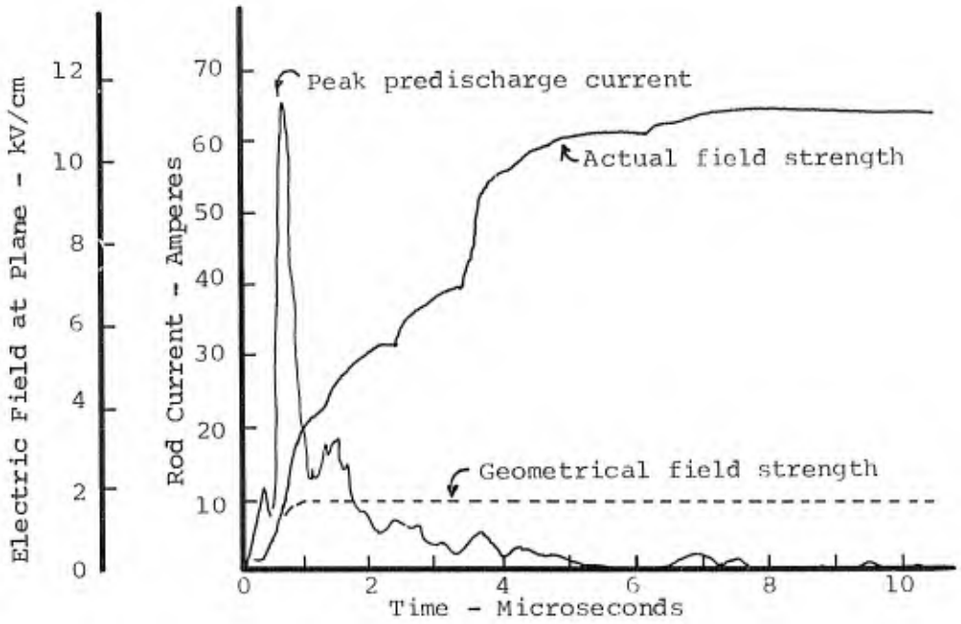

B. Gap Breakdown

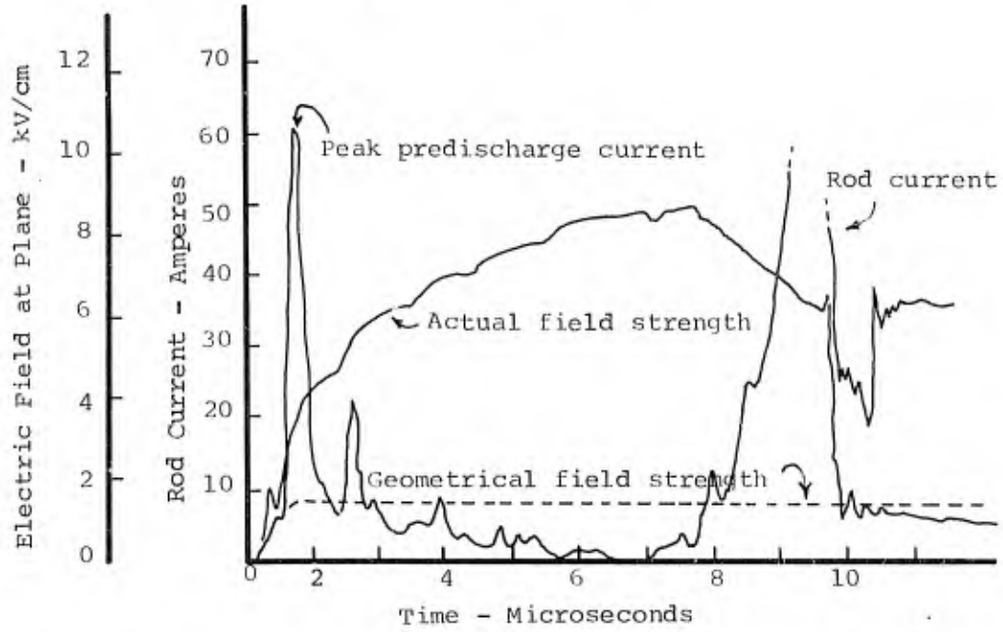

FIGURE 11 - Current and Electric Field Strength In a 150-cm Rod to Plane Gap (Critical Breakdown Voltage = 1360 kV - Negative Polarity)

The results obtained are plotted in Figure These charges are lower than those measured by Gallimberti, Rea, and Baldo for two reasons; these tests were made at a lower voltage than they used and the charge was measured at a grounded rod rather than at the high voltage electrode. A substantial number of the electric field lines from the high voltage electrode terminate on the grounded box rather than on the low voltage electrode.

With both polarities the charges increase with voltage level and the charge magnitude is different depending upon the polarity. This is due to the different mechanism of the particles movement with different polarity. As a matter of interest, however, when the charge is evaluated in terms of the percentage of total voltage required to give breakdown of the gap, the charge is about the same. The same effect was noted when measuring the electric field strength. The two effects are in reality one and the same; electric field is proportional to the charge in the gap and breakdown occurs when the gap is sufficiently ionized by the charge in the gap.

All the values were calculated from withstand tests. When a flashover occurs the charges can be much higher. Values of 41 μC and 47 μC for positive and negative polarity respectively were reached during the final electron avalanche leading up to breakdown. After breakdown occurs the total charge transfer depends only on the short-circuit current of the impulse generator, not upon the conditions in the gap.

2.3.5 Discussion of Test Results

The preceeding test results can be explained when the simplified circuit of a lightning arrester is considered. Two different parts can be distinguished, Figure 13. First is the main gap G of the arrester, along with the arc rotation coil which bypasses the current to ground and second is the RC circuit for transmission of RF energy.

The rated parameters of the lightning arresters are respectively

	L.A. #1	L.A. #2
Capacitance C	2000 pF	2000 pF
Resistance R	1.5 Mn	1 Mn
Capacitance gap G	20.5 pF	21 pF

The flashover characteristic of the gap G changes with the wave of the applied voltage and because the voltage between A and ground depends upon the variable conditions of the space surrounding the antenna, its performance cannot be predicted simply in terms of the applied voltage magnitude, either when

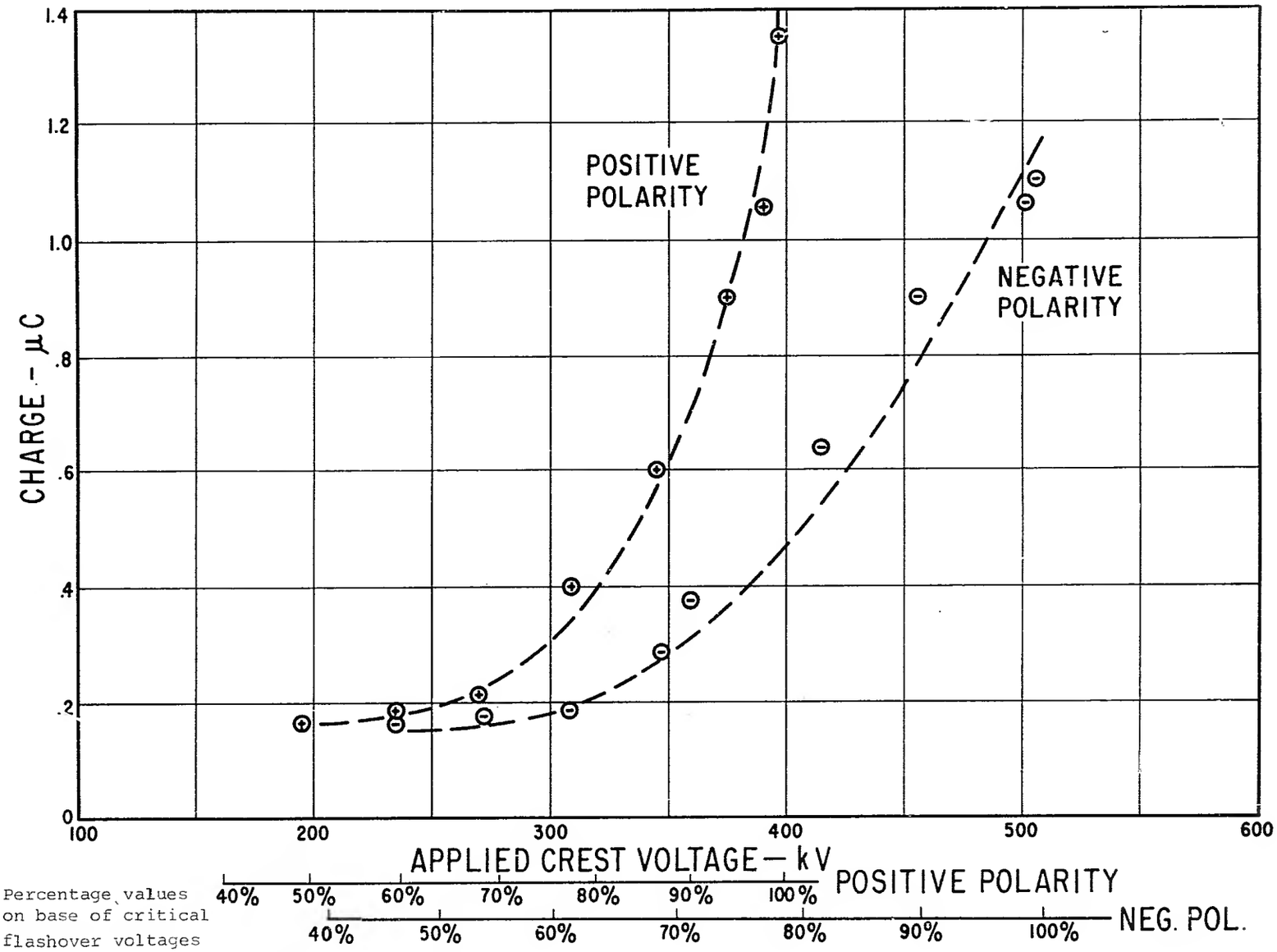

FIGURE 12 - Total Charge Transferred to Lower Rod Versus Applied Crest Voltage For Positive and Negative Polarities

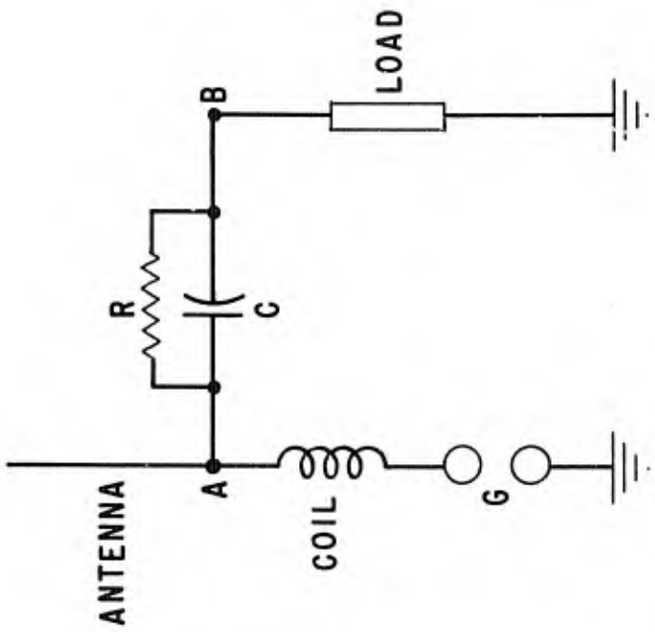

FIGURE 13 - Simplified Circuit of Tested Lightning Arresters

voltage is applied directly from a test generator or induced by a developing lightning flashover. To have, however, an idea of the flashover, the curves of the flashover voltage versus time to flashover for an impulse applied directly to the antenna were determined on both the arresters with positive and negative polarity as indicated on Figures 14 and 15.

With these elements in mind, the following reasoning applies when a resistor load is considered. As an impulse is applied to the main gap, the point A increases its potential level because the gap can be regarded as a capacitance divider, whose external terminals are the high voltage electrode and the ground. The charge that arrives at A depends upon the voltage level. Some of the charge is drained to ground through the gap G and some charges flow through the capacitor C. When a voltage small in comparison to that one that sparks the main gap is applied, the charge that arrives at A is of short duration and depends only upon the rapid rise of the applied voltage. Because no other bursts of charge arrive immediately, the capacitor C discharges completely through the resistance R and to ground and through the capacitance of the gap. As this charge flows through the resistor it produces a voltage pulse of constant duration since the waveshape of the current pulse is controlled by the waveshape of the high voltage impulse.

When the applied voltage is increased, some streamers can reach the lower rod and other charges arrive at A. These charges are delayed in comparison to the first ones as can be seen from the current oscillograms where some peaks start after the first one. The capacitor C is charged and discharged again and a second peak of voltage can be seen across the load. Depending on the form of the delayed pulses of the current, that is, depending on the number of pulses and on the times at which the charges arrive at A, the second impulse of the voltage across the load is formed with one, two, or more peaks. The higher the applied voltage, the higher are the peak values and shorter the time interval between pulses.

During all these conditions the voltage applied to the gap G will not yet be enough to spark the gap. Measurements have shown the gap voltage to be always higher than that across the load. This is logical because the capacitor C and the load act as a divider. Eventually the pulses of current have enough amplitude and are so closely spaced that they charge the capacitor to a high enough voltage to cause the gap to sparkover and divert the surge current to ground. If the capacitance is 2000 pF and the gap flashover voltage is 20 kV, this will occur when 40 μC has passed through the capacitor ($Q = CV$). Since

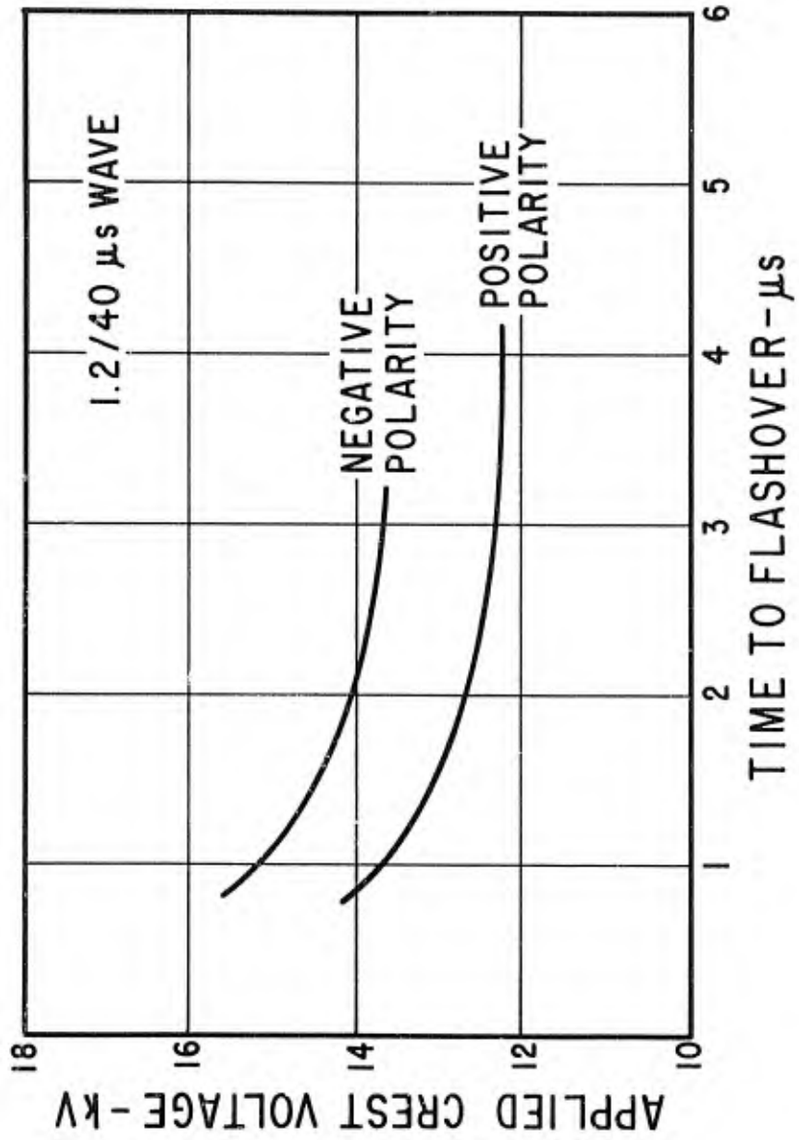

FIGURE 14 - Flashover Voltage Versus Time to Flashover for Lightning Arrester #1

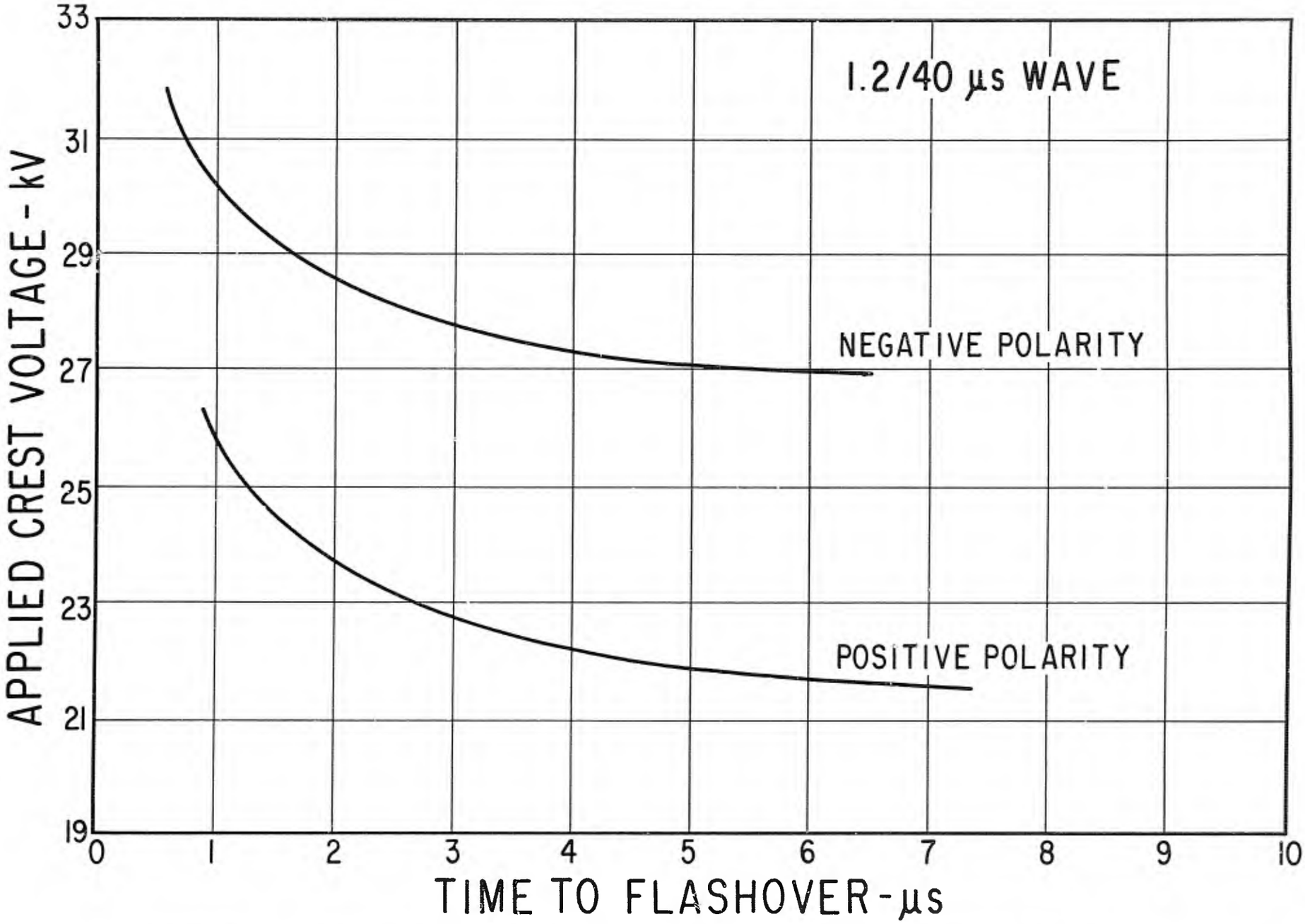

FIGURE 15 - Flashover Voltage Versus Time to Flashover for Lightning Arrester #2

the capacitor integrates its variable charging current, it follows that the voltage across the arrester gap will build up slowly in a series of steps taking perhaps many microseconds to reach a level that causes the gap to spark over.

Some measurements were taken of the voltage across the arrester gap (as contrasted to the previous measurements taken across the load) that show the stepwise buildup very clearly. These are shown on Figure 16. The time between application of the voltage to the external gap and breakdown of the internal gap of the arrester is 4 - 5 microseconds. The final stage of breakdown of the external gap leads to the steadily increasing voltage on the arrester gap. This final breakdown stress takes 1 - 2 microseconds. A long trailing wire antenna would collect much more charge, but collect it over a longer period of time.

When a tuned circuit is used, the mechanism described before still remains valid, but the circuit response is different, because of the change of the circuit parameters. The appearance and the sequence of the impulses of charge is the same as before, but one part of the charge pulse now passes to ground through the inductance of the tuned circuit and the other part charges the capacitance of the tuned circuit. The charge on that capacitance then discharges through the inductance, giving the characteristic damped oscillation noted on the oscillograms. In all cases the voltage will be less than if a resistance termination were used. The higher the frequency of the tuned circuit, the less will be the voltage produced by a given pulse of charge.

2.4 Conclusions and Implications

These tests have shown that breakdown, either of the air around the aircraft or of an aircraft lightning arrester is not an instantaneous affair. The breakdown process rather takes many microseconds, and perhaps in an aircraft many milliseconds. A breakdown process will probably be underway whenever the electric field strength on smooth surfaces of the aircraft reaches values on the order of 1000 volts per centimeter (100,000 volts per meter). The field strength around protruding objects on the aircraft will be much higher, though probably limited to around 500 kV per meter. A field strength of 500 kV per meter is a good rule of thumb as the voltage that will cause breakdown within a few microseconds between rod-shaped electrodes in air. Any time the applied voltage across a gap exceeds an average value of 500 kV per meter, there will be intense ionization in the gap. The charge generated in the gap will tend to limit the average electric field strength.

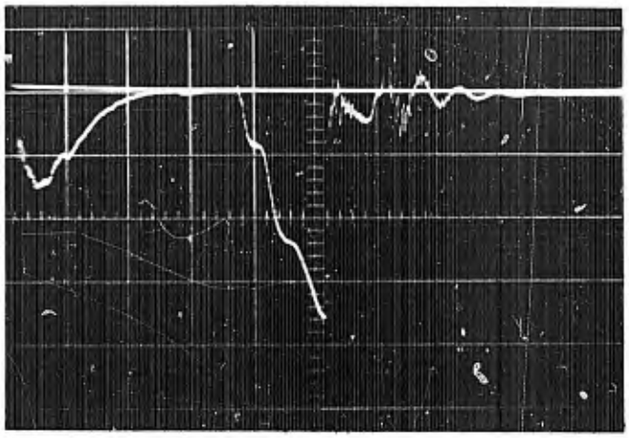

9.75 kV/div. 1 μs/div.
(a) Negative Polarity

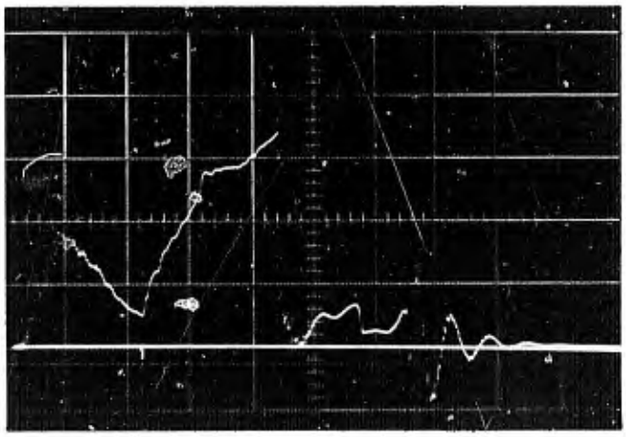

7.3 kV/div. 1 μs/div.
(b) Positive Polarity

FIGURE 16 - Oscillograms of Stepwise Build-Up of Voltage Across Internal Gap of Lightning Arrester During Flashover Test of Main Gap

The above assumes sea-level conditions. At higher altitudes the air pressure is less, and breakdown will occur at lower voltages. Most lightning strokes occur at altitudes less than 10,000 feet and even there the atmospheric pressure is still about 70% of sea level pressure. It would appear that the electric-field gradient around an aircraft should not exceed 100 kV or 200 kV per meter during a lightning stroke, except at exposed edges.

This electric field will increase or decrease in a series of jumps with each jump taking several microseconds to be completed.

Implications of this changing electric field as regards electromagnetic interference (EMI) or electromagnetic shielding will be discussed later in the report.

As regards avionic equipment connected to an antenna, one should design this equipment in the knowledge that it will be subjected to continuing pulses of current during the prebreakdown stage of the lightning flash. The individual pulses of current will have durations of about a microsecond and will transfer charge of the order of a microcoulomb. The voltage that will be produced by these pulses of current will depend on the nature of the avionic equipment. The lower the impedance of the avionic equipment, the lower will be the voltage produced by the flow of these currents. Voltages in the range 1 - 20 kV (or greater) were observed across a high resistance (10,000 ohm) load. Voltages across a tuned circuit were less, but still as high as 10 kV under some conditions.

The total charge transferred to the simulated antennae reached values of 40 - 50 μC during the final stages of breakdown of the simulated lightning stroke. The current that flows in this predischarge stage must charge the series capacitor of the lightning arrester. This capacitor thus must be insulated for sufficient voltage that it will not be damaged by charge that can build up prior to breakdown of the main gap of the arrester.

The voltage to which the gap is subjected will probably increase over a period of many microseconds. Thus it would appear that the gap breakdown strength should be evaluated with a test wave rising to crest in (perhaps) 10 - 100 microseconds.

SECTION 3

3.0 Electrical Characteristics of Simulated Lightning Flashes

This section deals with the electromagnetic environment to which an aircraft will be subjected if it is hit by lightning. Most of the material in this section deals with a series of measurements made to determine the frequency spectrum of radiation from a four-meter arc.

3.1 Measurements

Measurements were made using an RFI meter and antennas 20 ft. away from a four-meter arc produced between two rod-shaped electrodes. Figure 17 shows in semidiagrammatic form the type of test circuits and the positions of the various circuit elements. The arc was produced by the HVL's outdoor impulse generator. The voltage applied to the gap was measured by a resistance-capacitance voltage divider rated at 5000 kV for impulse voltages.

Field intensity was measured at a point in space about as close to the arc as it was safe to place the antennas of a radio interference meter. The antennas were placed atop a pole at a height of about 22 ft., on the center line of the four-meter arc. The signals were coupled through a 50-ohm surge impedance cable to the RFI meter located in a screened enclosure. Resistance attenuators were used to reduce the signal level from the antennas to a level that could be measured by the RFI meter.

Several different types of antennas were used, depending on the frequency band under investigation. These included a whip antenna and a long antenna; also bi-conical and log-conical spiral antennas.

The noise meter used was an Empire Devices Model NF-105 with a variety of plug-in tuning heads. The meter was operated in its PEAK mode of response since this allowed us to use the broadband (approximately 1 GHz) internal calibrator of the noise meter as a reference source of amplitude.

The principle of measurement was as follows:

1) Select the appropriate antenna and tuning unit.

2) Select the desired frequency of observation.

3) Set the input attenauator of the NF-105 to an appropriate level and insert an attenuator (or attenuators) in the lead connecting the antenna to the noise meter.

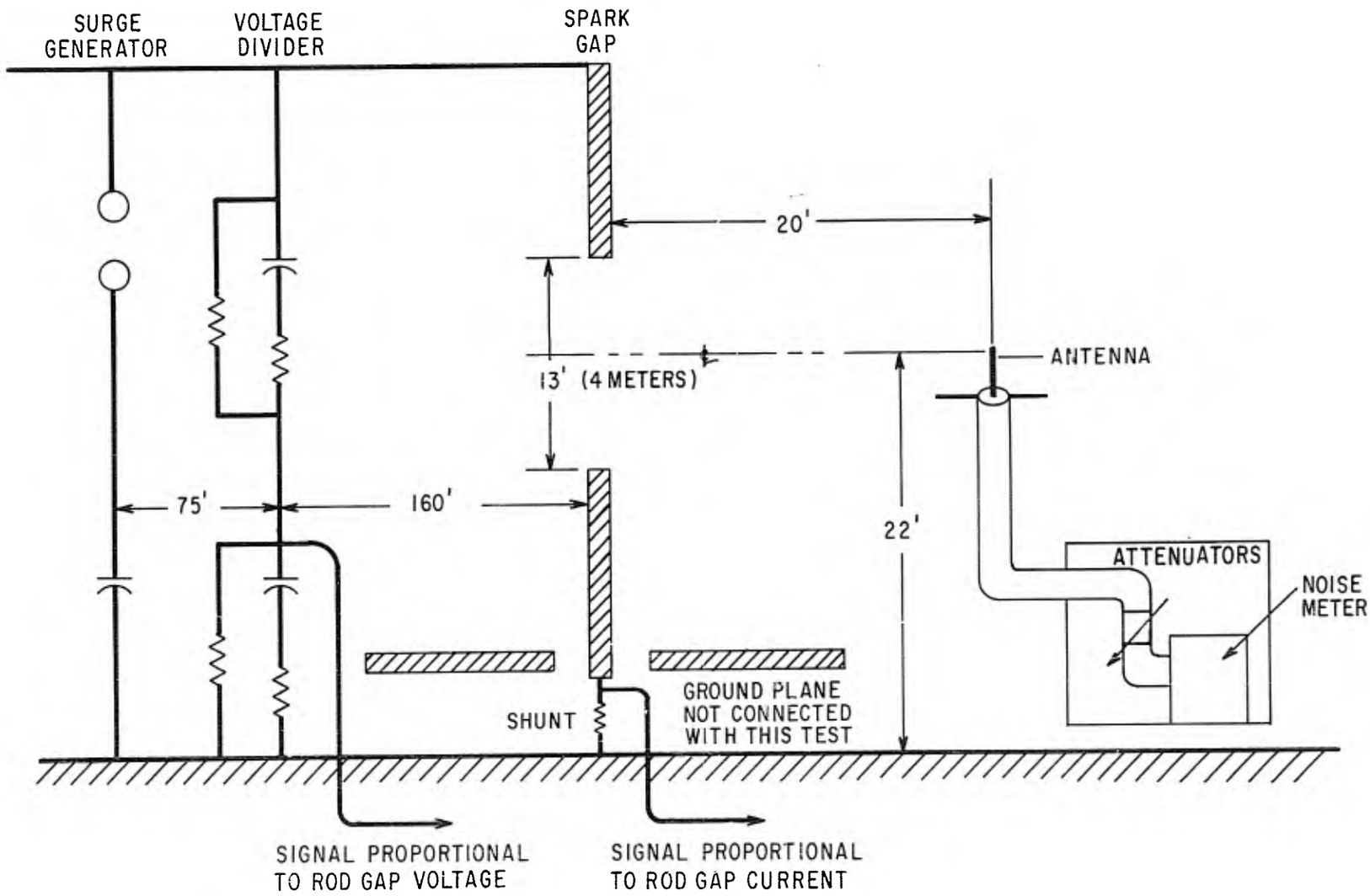

FIGURE 17 — Test Setup for Determination of the Electrical Characteristics of a Four-meter Arc

4) Using repeated shots of the impulse generator, adjust the IF gain of the noise meter until the noise from the electrical arc is just audible from the audio output of the noise meter.

5) Leaving the IF gain of noise meter set, connect the RF input of the noise meter to the calibrator output.

6) Adjust the attenuator and output level control of the calibrator until the audio output from the noise meter is just audible.

The output level from the calibrator will then be the same as the signal produced by the high voltage arc if all the attenuator factors are correctly considered. As an example, assume that the signal from the arc was measured with a 40 dB attenuator in the lead between the antenna and the noise meter. Further assume that a signal from the calibrator of 66 dB (relative to 1 μV MHz bandwidth) produced the same barely audible signal from the receiver as did the electrical signal from the arc. The spectral density of the signal applied to the noise meter at that particular frequency would then be 66 + 40 = 106 dB above 1 μV/MHz bandwidth. This would correspond to a spectral density of 200,000 μV/MHz, or 200 μV/ kHz bandwidth. This figure must be corrected for the antenna correction factor and the cable losses, if any, between the antenna and the noise meter. These are available from the manufacturer of the RFI instrument. Assume the antenna factor is 40 dB and the cable correction factor is 6 dB. The spectral density of the field at the antenna location would then be 40,000 μV/meter per kHz bandwidth.

3.2 Results

The results of the measurements are shown on Figure 139. The tuning heads used in the NF-105 meter and the type of antenna used for each band are shown on the curve. The results generally follow a logical curve, at least over the range 100 kHz - 1 GHz.

The measurements show a definite peak at 400 kHz. The impulse generator-rod gap circuit does oscillate near that frequency when the gap flashes over and the signal level at that frequency should be high. In an actual lightning flash, the current would not be oscillatory and no such peak should occur. No unusual peaks of radiation were detected at the higher frequencies and the data in general looks good. The high-frequency fall-off rate would appear to be about 50 dB per decade.

At lower frequencies, the data seems suspect. At 20 kHz the indicated field strength is 300 dB relative to 1 μV/meter per kHz bandwidth, or 10^9 V/meter per kHz

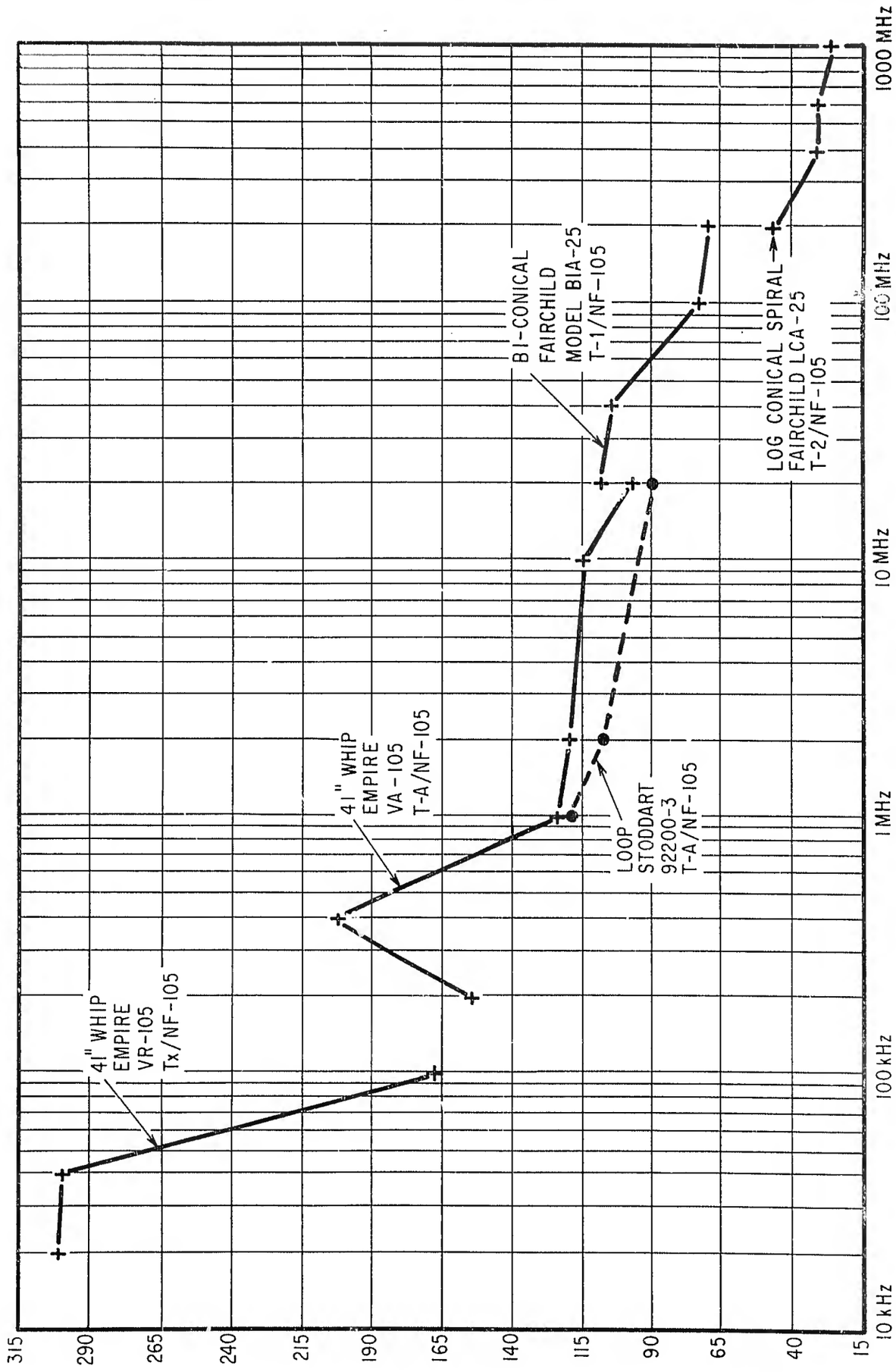

FIGURE 18 - Spectral Density of the Field Associated with a High Voltage Arc

bandwidth, a completely unrealistic measurement result. Since external attenuators had to be used on the antenna signal to prevent overloading, it is most probable that the cascade series of attenuators did not work properly. The same data is plotted on a different scale on Figure 19 to allow a comparison with the data of Oh, et al.[1]

Of more importance than absolute magnitude is the slope of the spectral amplitude vs. frequency curve. Both curves seem to show a $1/f$ relationship in the vicinity of 1 MHz and a break to a faster slope around 100 MHz.

Figure 20 shows the waveshape of the voltage across the gap and the current through the gap. Breakdown of the gap and the heavy flow of current occurs at 10 microseconds, though this time varies from shot to shot.

Some oscillograms of the output of a loop antenna employing different band pass filters were also taken. This data is shown on Figure 22. At low frequencies, the output from the antenna appears to be that magnetically induced by the flow of current in the impulse generator and rod gap circuit. This current is greatest when the rod gap arcs over. As expected, the output from the antenna is greatest at the time the rod gap arcs over. At higher frequencies, an output is noticed even before the electrodes arc over. An output of similar character, but greater amplitude, is observed when breakdown occurs. This initial output is doubtlessly caused by leaders that develop prior to complete breakdown of the gap.

This broadband data is in rough agreement with the narrow band data shown on Figures 18 and 19. As an example, in the range from 150 to 305 kHz, the average field strength would be about 170 dB, or 300 V meter per kHz bandwidth. Averaged over a 150 kHz band, this would correspond to 45,000 V/meter. The direct output of the loop antenna was 10 Volts peak. Adding the antenna correction factor of 60 dB (approximately) the peak electric field strength would then be 10,000/volts meter averaged over a 155 kHz bandwidth.

No attempt has been made to scale this data for distance away from the arc, but certainly the electric field strength at the antenna location will be less than that in the gap itself. In the gap, the field strength was about 600 kV meter.

1. Luis Oh, George Huang, Reuben Goldman, et al. "Natural and Induced Electrical Effects on Integrated Antennas and Circuits at Frequencies to 10 GHz". Report AFAL-TR-69-210

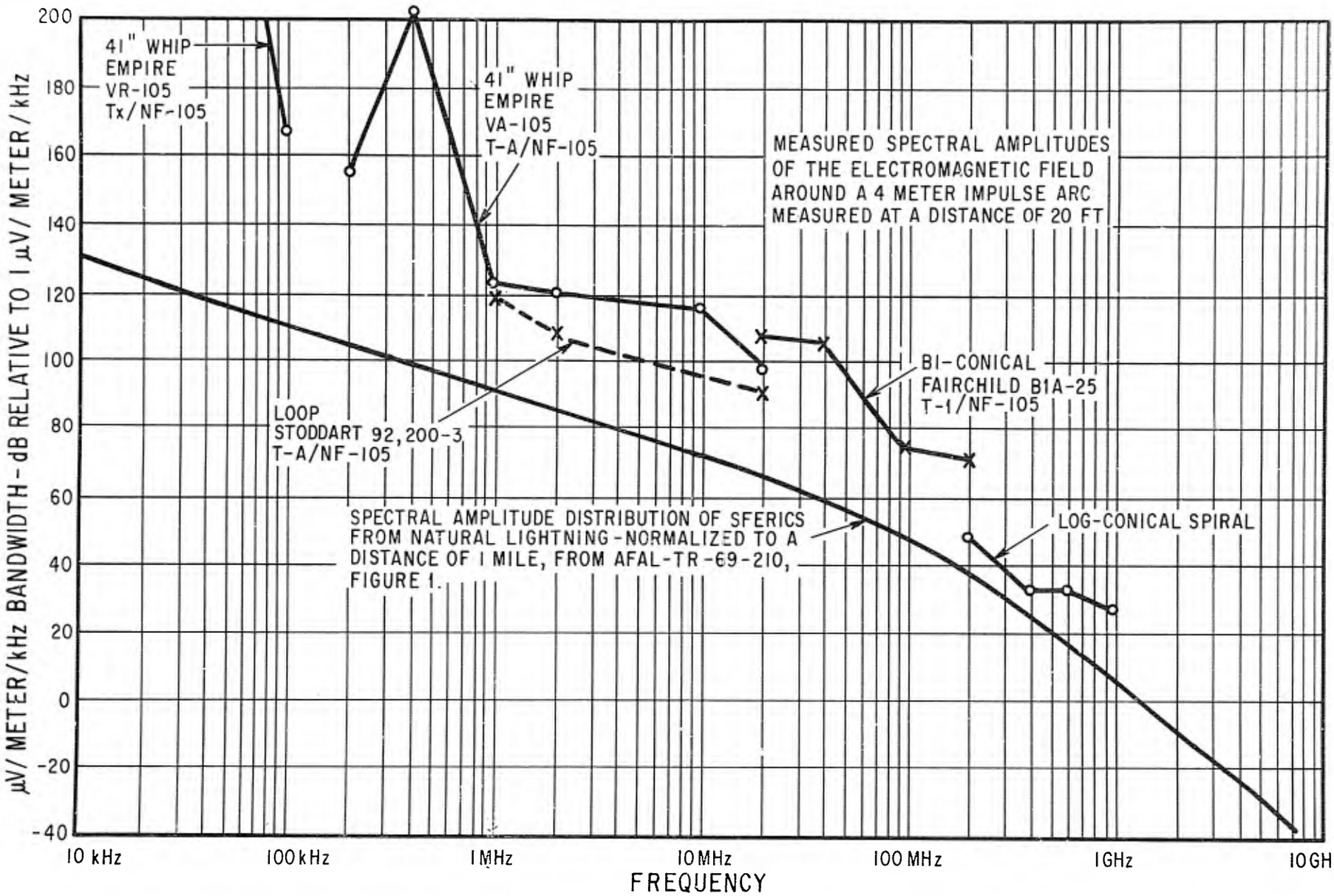

FIGURE 19 - A Comparison of Measured and Observed Spectral Amplitudes

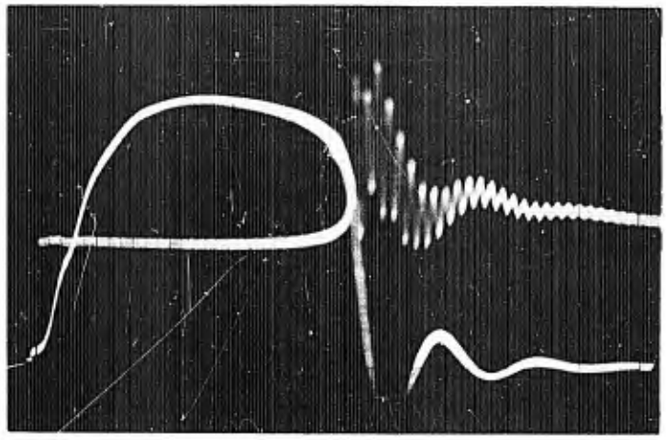

Voltage Trace - 618 kV/div 2 μs/div
Current Trace - 2100 A/div 2 μs/div

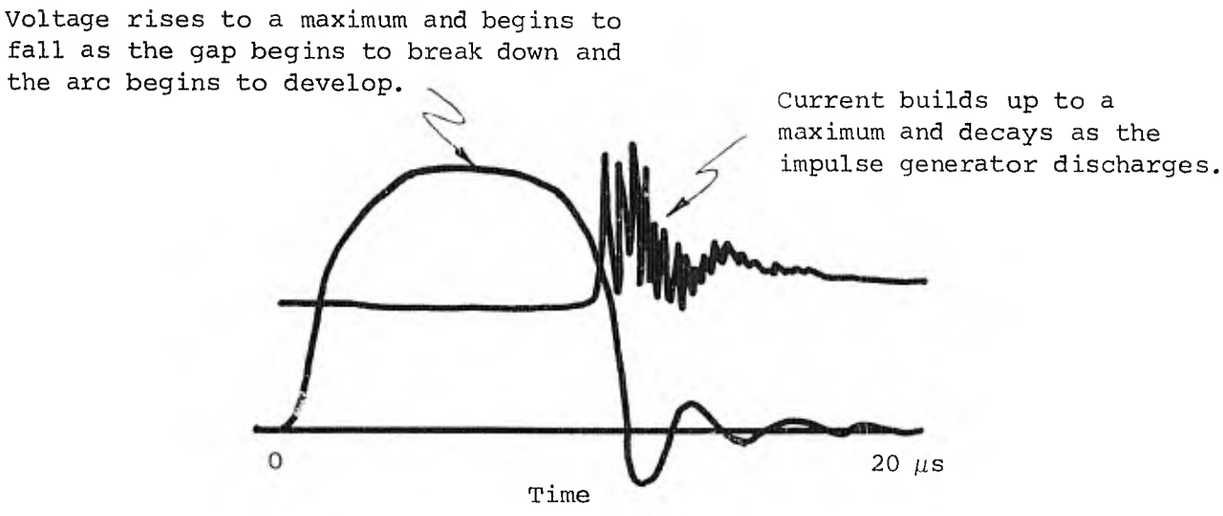

FIGURE 20 Voltage Across, and Current Through, the Four-meter Arc

A. 150-305 kHz Band

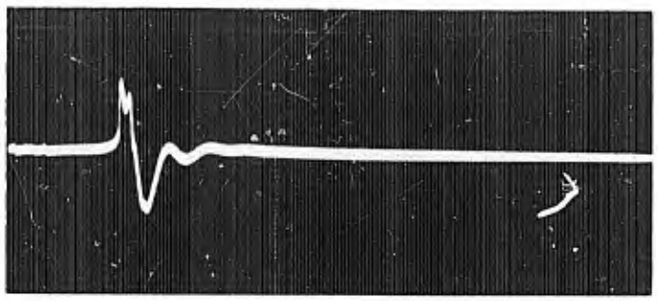

10 V/div 5 μs/div

Essentially all the output occurs at the time of arc development.

B. 1.1-2.25 MHz Band

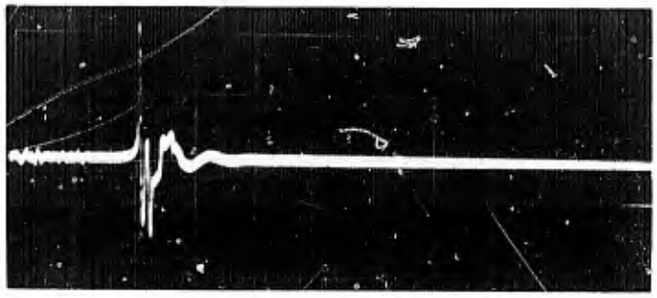

10 V div 5 μs/div

Essentially all the output occurs at the time of arc development.

C. 15-32 MHz Band

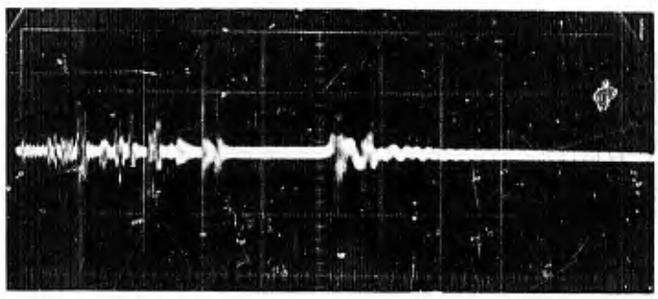

1 V/div 2 μs/div

Significant outputs occur even before the arc develops.

FIGURE 21 — Loop Antenna Outputs in Three Different Frequency Bands

At the antenna location, the field was probably down by an order of magnitude, perhaps in the range from 30,000 to 60,000 volts per meter, a figure in agreement (within an order of magnitude) with that actually measured by the antennas either on a broad-band or narrow-band basis.

The measurements of electric field strength during the tests on the simulated lightning arresters showed that the electric field strength at the surface of a plane surface close to a point of attachment of the arc would probably not exceed 100 kV meter. This would correspond to the lower frequency regions, on the order of 100 kHz bandwidth. Taking 100 kV meter at 100 kHz as a base and using the slope of the curve of Figure 140, one might expect the field intensity vs. frequency to be as shown in Table VI.

TABLE V

Expected Maximum Spectral Density of Field Strength on a Plane Surface Near, But Not At, the Point Of Attachment of a Lightning Stroke

Frequency	kV/Meter per 100 kHz bandwidth	Volts/Meter per KHz bandwidth
100 kHz	100	1000
1 MHz	10	100
10 MHz	1	10
100 MHz	.1	1

SECTION 4 -

4.0 Blast Energetics of Sparks

4.1 Introduction

The pressure wave from a lightning flash will travel away from the flash at a velocity proportional to the energy liberated by the flash. Near the flash, shock-wave conditions will prevail and the wave will propagate at a velocity greater than the normal sonic-propagation velocity. The velocity of propagation depends on the overpressure, $\Delta P/P_o$, or the degree to which the shock-wave pressure front exceeds the normal pressure in the medium. An extensive body of literature is available relating propagation velocity to overpressure. Thus measurements of the time of arrival of a shock wave at a point can be related to shock-wave theory to yield the overpressure at that point.

The type of shock wave produced by the lightning discharge is of interest for the explanation of thunder (Few, 1969)[1] as well as for the estimation of shock damage to structures such as aircraft. The paucity of natural lightning measurements has led to laboratory experimentation with sparks. Presently, there appears to be little agreement in the literature on the shock-wave shape (cylindrical or otherwise) produced by sparks (Few, etal. 1970).[2] In part, the problem is related to the erratic paths followed by sparks and to the rapid decay of shock waves propagating into sea-level air. Specifically, the shock-wave measurements must be made near the channel, although often the spark location cannot be accurately specified from shot to shot. Further, the extremely high voltages generated make close-in measurements difficult to achieve.

The purpose of this section is to present results on measurements of shocks from a 25 cm spark in air and to show that close-in measurements may be made on long (382 cm) sparks. We find that approximately one percent of the total capacitor energy is utilized by the mechanical shock. Curiously, there is no significant difference in the energy measured in the spark from a highly oscillatory discharge and that from the same device critically damped. Visual observation of the sparks indicated numerous occasions of splitting. Measurements on split sparks did not show a significant difference between

---

1. Few, A.A., Power Spectrum of Thunder, J. Geophys, Res. 74, 6926, 1969.

2. Few, A.A., H.B. Garrett, M.A. Uman, and L.E. Salanave, Comments on Letter by W.W. Troutman "Numerical Calculation of the Pressure Pulse from a Lightning Stroke", J. Geophys, Res. 1970

them and the unsplit ones. Hence, these results provide no support for the 'tortuosity' theory of Few (1969).

4.2 Theory

Blast-produced shocks from line-like sources should be cylindrical until the propagation distance is of the order of the line length. A slow transition to the spherical case then ensues. In either case, the trajectory equation is one dimensional and for the cylinder is written (Jones, 1968).[3]

$$T = \tfrac{1}{2}\left[(1 + 4X^2)^{\frac{1}{2}} - 1\right] \qquad \text{Eqn. 4-1}$$

where

$$T = \frac{a_o t}{R_o}$$

$$a_o = 3.4 \times 10^4 \text{ cm} \times \text{s}^{-1}$$

$$R_o = \left(\frac{4E_o}{B\gamma P_o}\right)^{\frac{1}{2}}$$

E_o = Energy

P_o = Pressure

$\gamma = 1.4$

$B = 3.94$

$X = R/R_o$

R = Distance from axis, reached in Time t

The significance of Eqn. 4-1 is that simultaneous measurement of arrival time and distance permits solution for E_o, the energy in the mechanical shock; thus,

$$E_o = \frac{B\gamma P_o}{4}\left\{\frac{R^2 - a_o^2 t^2}{a_o t}\right\}^2 \qquad \text{Eqn. 4-2}$$

From Jones (1968), we can now map the overpressure field of the shock:

$$\frac{\Delta P}{P_o} = \frac{\gamma}{\gamma+1}\ \frac{1}{2}\ \frac{1}{0.555\left[(1 + 4.8\ x^2)^{3/8} - 1\right]} \qquad \text{Eqn. 4-3}$$

Both Eqn. 4-1 and Eqn. 4-3 have been experimentally verified. We will later need the exact shock-jump relation

$$\frac{\Delta P}{P_o} = \frac{2\gamma}{\gamma+1}(M_x^2 - 1) \qquad \text{Eqn. 4-4}$$

---

3. Jones, D.L., Intermediate Strength Blast Wave, Phys. Fluids 11, 1664, 1968a

where M_x is the normal shock Mach number. In terms of known parameters, we can write the pressure of the reflected shock

$$\frac{P_r}{P_o} = \frac{\left[(3\gamma - 1)\ M_x^2 - 2\ (\gamma - 1)\right]\left[2\gamma M_x^2 - (\gamma - 1)\right]}{(\gamma^2 - 1)\ M_x^2 + 2(\gamma + 1)} \qquad \text{Eqn. 4-5}$$

To estimate the ionization in the blast wave, we could calculate the temperature from the Rankine-Hugoniot relations. Such procedure is notoriously unreliable; instead, we use the detailed tables of Gilmore (1955).[4]

Lastly, we use the Saha equation for ionization equilibration to calculate the ionization levels created by the shock. To first approximation,

$$\alpha = 0.78\left[\frac{P_T}{T^{5/2}} \times \frac{9}{2} \times 10^4\, \epsilon^{\frac{169000}{T}} - 1\right]^{-\frac{1}{2}} + 0.21\left[\frac{P_T}{T^{5/2}} \times \frac{8}{9} \times 10^4\, \epsilon^{\frac{158000}{T}} + 1\right]^{-\frac{1}{2}} \qquad \text{Eqn. 4-6}$$

where α is the ionization fraction and P_T is the pressure in Torr.

4.3 Experimental

Measurements were made by placing a piezoelectric microphone near a high voltage spark and displaying the output on an oscilloscope. If the oscilloscope is triggered by the electrical disturbance producing the arc, the oscilloscope displays directly the time of arrival of the shock wave at the microphone. Two types of measurements were made: one in which the microphone was coupled directly to the oscilloscope (Figure 22) and one in which the microphone was coupled optically to the oscilloscope (Figure 23). If the microphone is coupled directly to the oscilloscope, it is at ground potential. If placed too near the high voltage electrodes, the spark will jump to the microphone and not between the electrodes. This may not damage the microphone, but it does limit how close one can get to the spark.

During this series of measurements an optically-coupled type of measurement was also made. The microphone, through a buffer amplifier, drove a light-emitting diode. The light output from this diode was coupled via a fiber optic light pipe to a photomultiplier, the output from which was then displayed on the oscilloscope. With this arrangement the microphone can be placed within a few centimeters of a spark without significantly interfering with the spark.

Two different spark generators were used. Both are standard (Marx) types, charged in parallel at low voltage and discharged in series at high voltage. Unit 1, located indoors, for which we have the most data, was discharged at 200,000 volts through a 25 cm gap. Total energy stored was 26,666 Joules.

---

4. Gilmore, F.R., Equilibrium Composition and Thermodynamic Properties of Air to 24,000 ^{o}K, The Rand Corporation, Report Rm 1543, August 1955.

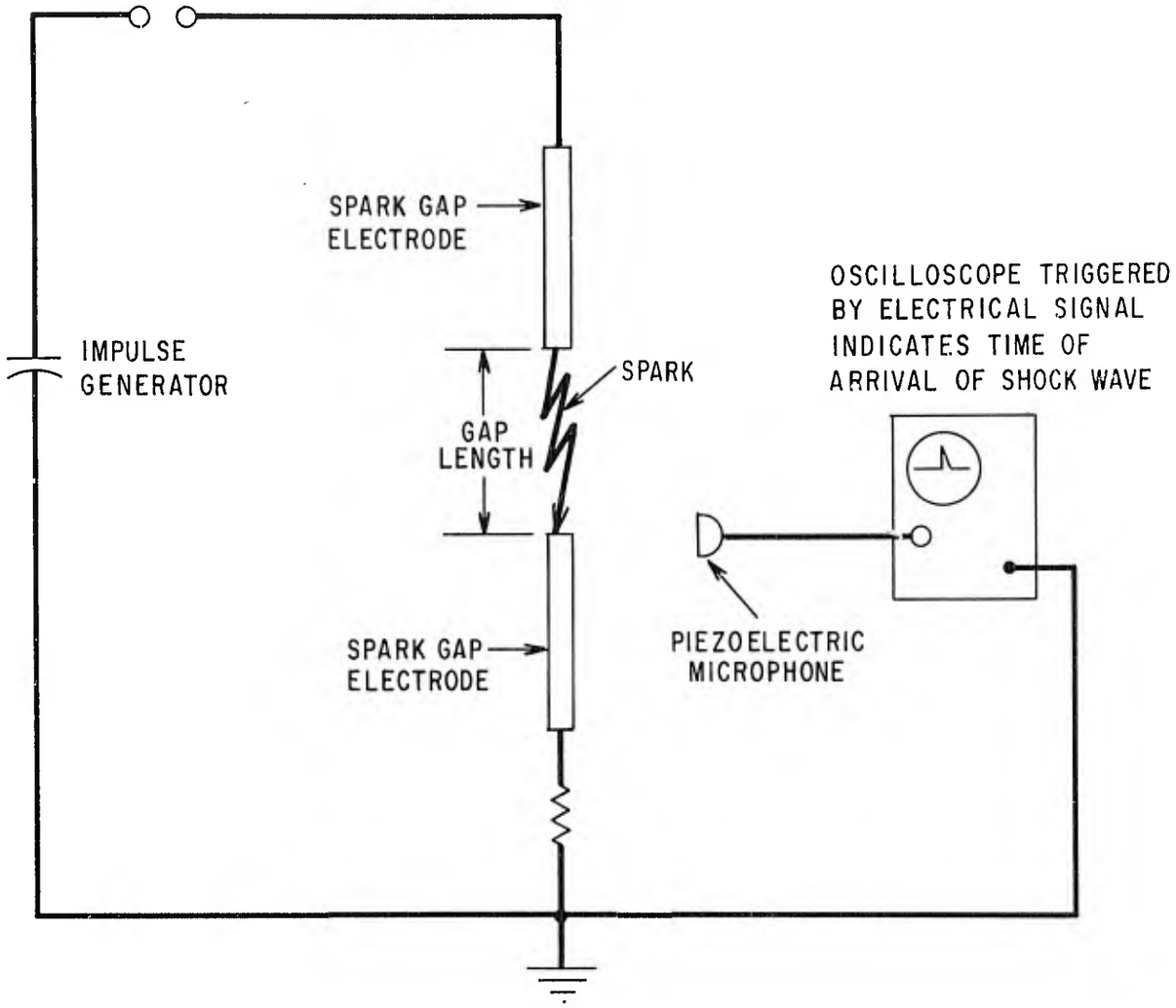

FIGURE 22 - Directly-Coupled Microphone For Measurement of Shock-Wave Arrival Times

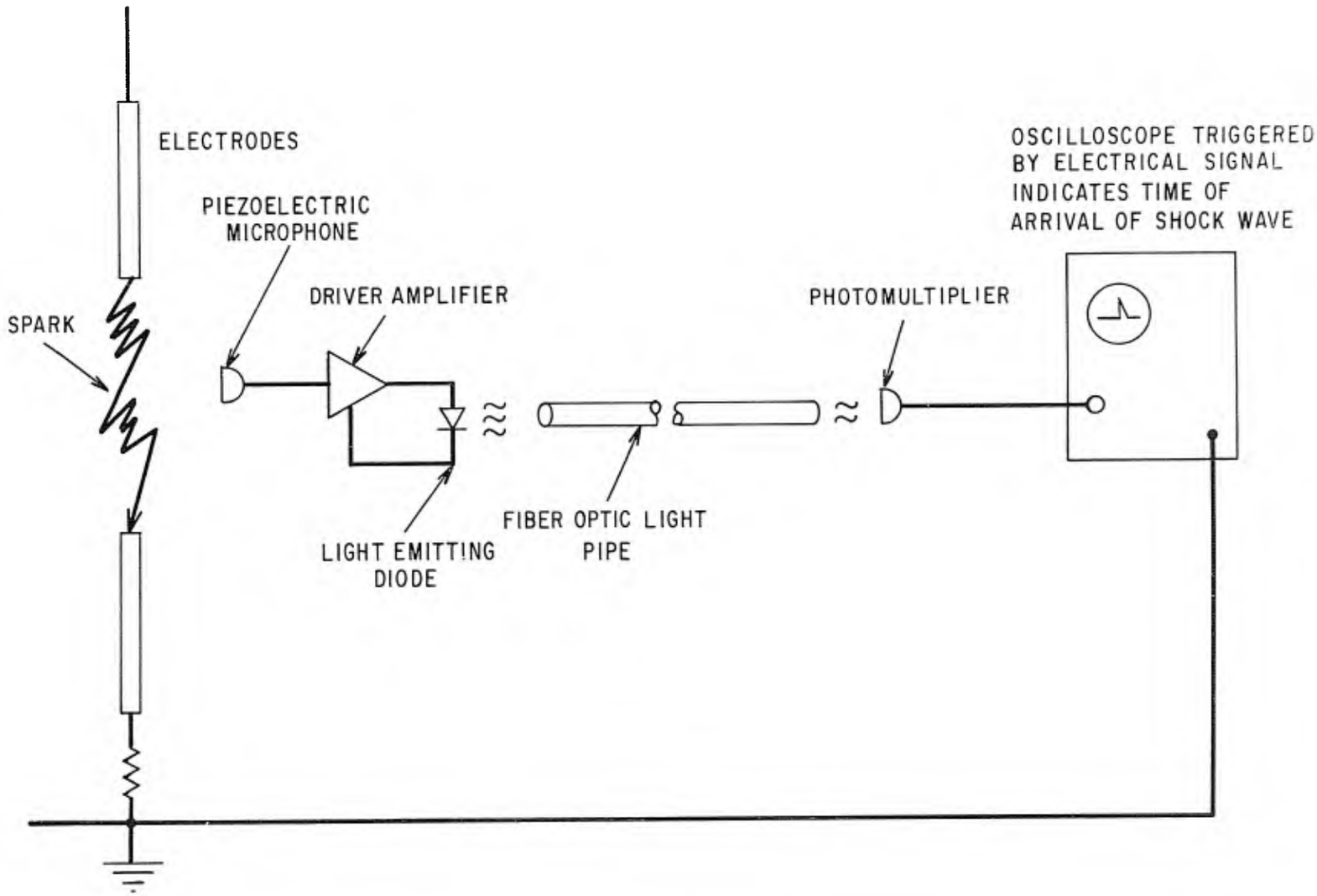

FIGURE 23 - Optically-Coupled Microphone Than Can Be Placed Very Near a High-Voltage Spark for Measurements of Shock-Wave Arrival Times

Figure 24 shows the current waveform for two cases of damping in the circuit. On the left the discharge is highly oscillatory, with a period of approximately 0.7 microsecond. The traces below show arrival times at the probe from successive shots. On the right, with the circuit very nearly critically damped, the discharge takes almost one microsecond to reach current maximum. Again, below are pressure-waveform traces from successive shots.

Unit 2 was outdoors. It is the 5,000 kV generator which, for these experiments, was charged to 2,300 kV. It is rated at 250,000 Joules, but because of the reduced voltage, only 21 percent of this rated energy was available. The gap was set at approximately 12.5 feet or 382 centimeters. During these experiments, a stiff, gusty wind was blowing at an estimated 20 knots. The resulting movement of the upper and lower electrodes is estimated at 10 to 15 centimeters, maximum. Consequently, quantitative shock arrival measurements were not possible, because of the large uncertainty in X in Eqn. 4-1. All measurements were made with a standard piezoelectric probe of the type described by Jones and Vlases (1967).[5] Rise time of this probe is approximately 0.1 microsecond.

4.4 Data

As previously noted, data was taken with both grounded and ungrounded probes. For 25 cm gaps, columns A and B of Table VI are the arrival times of the shock wave at the grounded probe. Columns C and D of this table give the travel time to the probe when it was floating. The major difference in the two cases is the proximity accessible to the floating probe. When the probe was directly connected to the oscilloscope, it was not possible to get nearer than 10 cm without drawing the arc, even with the probe very nearly at the level of the ground electrode. With the probe at the midpoint of the arc, column B, strikes occurred as soon as the probe came within approximately one gap distance. However, by floating the probe, measurements as close as 4 cm became possible (column D). The difference between columns C and D is shown by the discharge waveforms of Figure 24. Shockwave output from the critically-damped discharge (D) is essentially the same as for the oscillatory discharge (A, B, C).

---

5. Jones, T.G., and G.C. Vlases, Pressure Probes for Research in Plasma Dynamics and Detonation, Rev. Sco. Inst., 38, 1038, 1967.

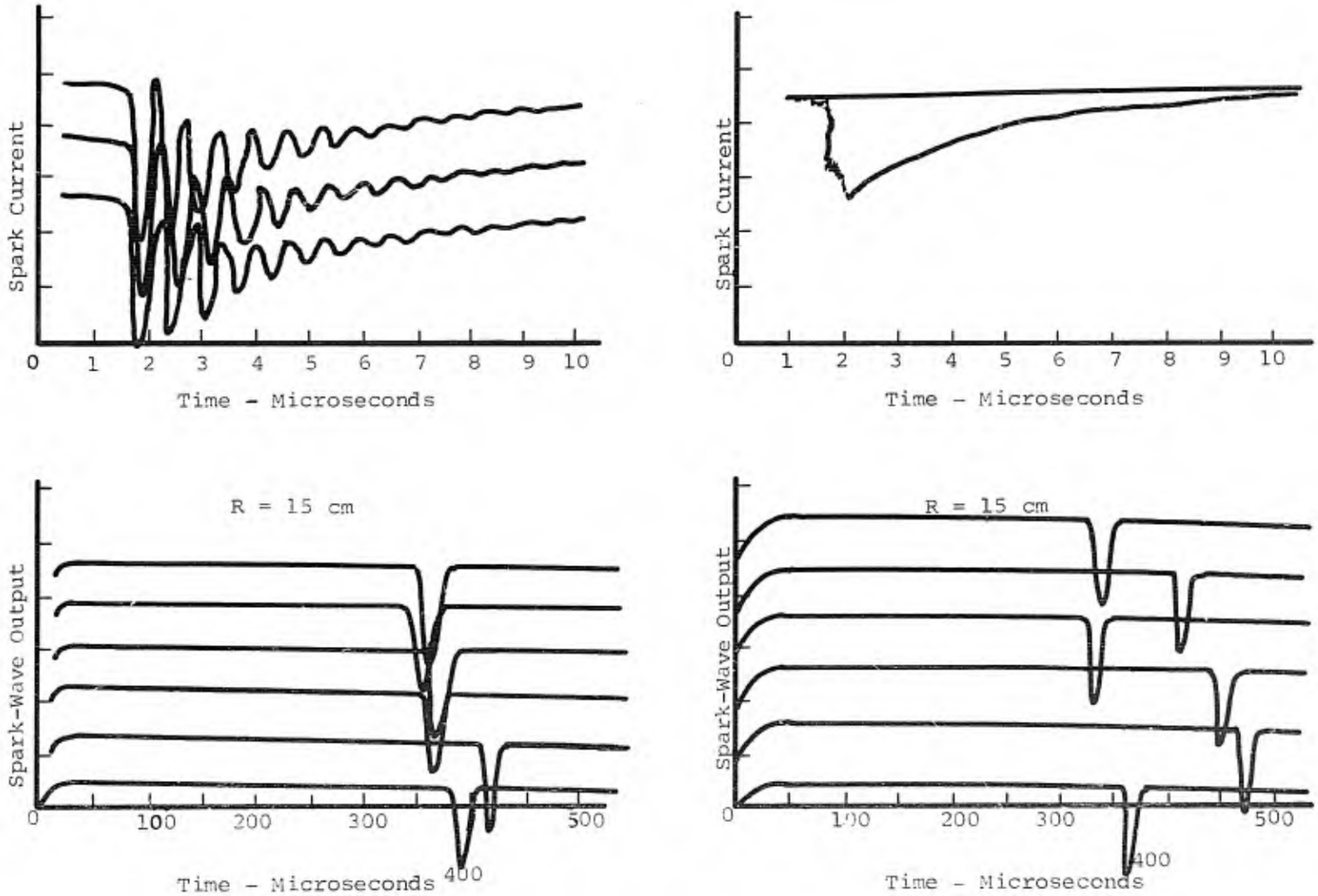

FIGURE 24 - Current and Pressure Waveforms of High-Voltage Sparks in a 25 cm Gap

TABLE VI

Collected Shock Arrival Times (Microseconds) from the 200 kV, 25cm Gap Discharge

R(cm)	A 1¼ cm Above Base	B Midpoint	C Kresge Midpoint	D Kresge Midpoint (damped)	Calc
4			Hit	100	
5					91
5			145	150	
7½					160
8	Hit		160	170	
10	263		253	200	231
12½	305		280	335	302
15	393		345	370	375
17½	410		448		447
20	515	Hit	505	550	520
22½	585	580			593
25	675	645	600	695	666
27½	740	720			739
30	830	800	790	810	813

The columns labeled Kresge represent measurements taken with the floating data system devised by J. Kresge of the G.E. High Voltage Laboratory. The posted numbers are the median values, usually from a set of five or more separate shots.

It should be pointed out that the data shown in Table VI are the median values of a group. That is, at each point five or more separate shots are taken, the arrival times are posted in order and the middle (or median) value is chosen to represent that group. This procedure is justified on the basis of the need to characterize an erratic phenomena. The spark is rarely confined to the path between the electrodes, often bowing, always showing jagged structure and sometimes splitting. An example of the shot to shot spread can be found in the two lower points of Figure 24. When measuring an arrival time (and hence inferring an energy), the actual distance traveled must be known for proper use of Eqn. 4-2. With a spectrum of radii (or times) to choose from, the mediam value better represents the correct case than does, say, an average, since the shock propagation is quasi-parabolic instead of linear. Table VII and the lower traces of Figure 25 represent the data from the spark discharging through the 381 cm gap. Unfortunately, high, gusty winds precluded the precise determination of location. Indeed, even relative location is probably not known to better than one or two centimeters. For these measurements, the probe was floating and was placed twenty centimeters above the base electrode.

4.5 Results

The principal result of this study is the graph shown in Figure 26. Here, all the data from Table VI is plotted for comparison. Although there is considerable scatter, as compared to the earlier data of Jones (1968) on other types of blasts, it is reasonable to conclude that the cylindrical blast wave line (solid, E_o = 3.3 J/cm) represents the data adequately. A dashed line is drawn for a spherical blast wave with the same energy. The spherical blast clearly does not encompass very many data points. Since every spark was observed to be "tortuous" to some extent, the evidence in support of the Few 'tortuosity' theory is lacking.

Curiously, the data from oscillatory discharges (Δ, 0, X) do not differ materially from those from the one that is critically damped (Y). The interpretation is probably that the bulk of the energy is released to the mechanical shock during breakdown, when the resistance of the channel is quite high. In other words, the I^2R integral is dominated by the current rise, when the air is still relatively resistive. After arc-over, the channel air is ionized; with a low resistance there is little energy transfer to the plasma. Some energy is certainly transferred to the gas during each succeeding oscillation as shown

TABLE VII

Shock Arrival Times (microseconds) from the 2,300 kV, 381 cm Gap Discharge

Z(cm)	t	t(median)
0	125	135
	130	
	140	
	150	
7.6	610	655
	635	
	675	
	910	
15.2	560	1040
	700	
	1000	
	1040	
	1160	
	1210	
	1240	
30.5	1280	1500
	1500	
	1600	

This distance Z is arbitrary in the sense that the location of the arc varied from shot to shot and group to group. Best estimate of the location of the probe at Z = 0 is 6 to 8 cm from the average arc path.

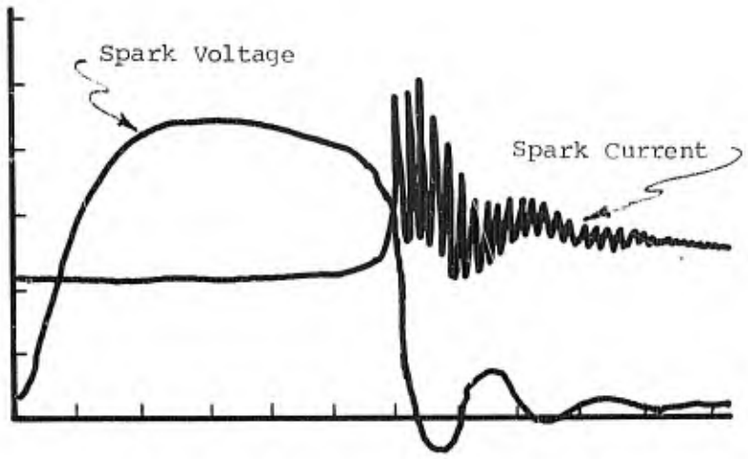

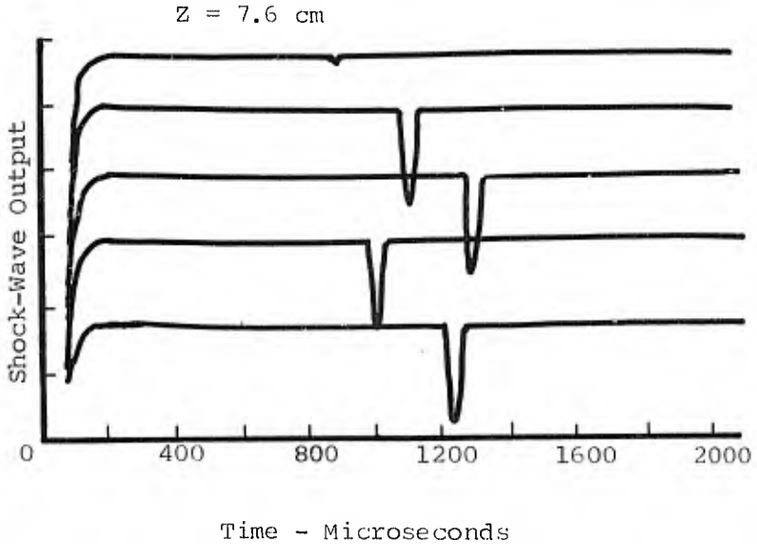

FIGURE 25 - Current, Voltage and Pressure Waveforms of High-Voltage Sparks in a 382 cm Gap

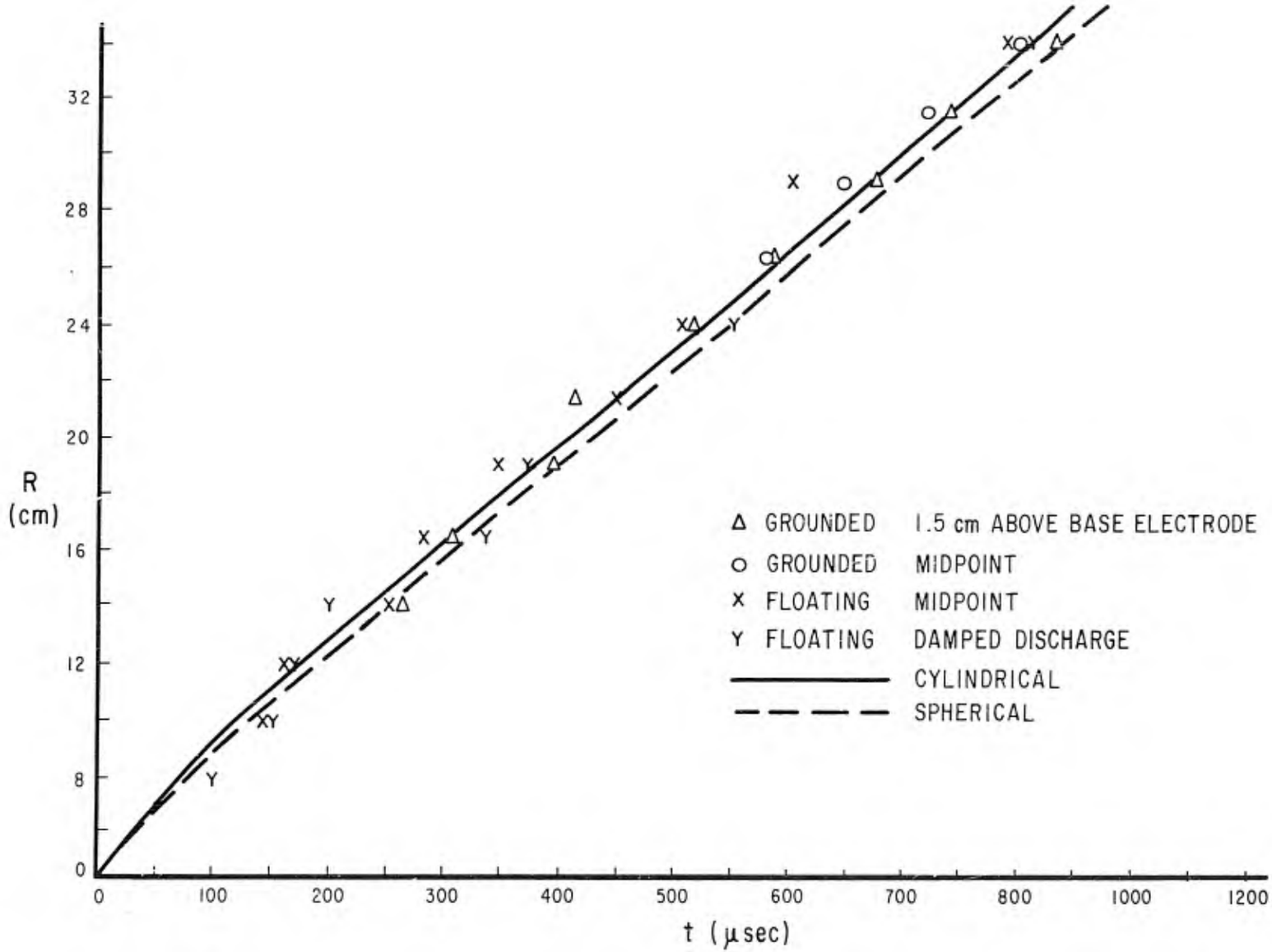

FIGURE 26 - Comparison of Experimentally Determined Arrival Times with Those Predicted by Cylindrical and Spherical Shock-Wave Theories

by Jones (1968b),[6] who measured the ionization from the ultraviolet pulse that accompanies each current maximum. However, this energy is small relative to the initial breakdown pulse. These experiments were not specifically designed to seek data on secondary shocks, but the data on both Figures 24 and 25 tend to show the absence of any large pressure oscillations following the first shock. In this respect we do not confirm the measurements of Uman et al. 1970,[7] who sometimes find several shockwaves. However, in terms of the gap scaling, we were not so far from the channel as they. A most important aspect of this work is the qualitative measurements made on the 381 cm spark gap. These data, shown in Figure 25 lower, prove the feasibility of making close-in (as well as far-out) measurements on very high voltage arcs. The simplicity of the system, i.e, a piezoelectric probe connected to the oscilloscope via an optical hook-up, makes precise determination of shock wave parameters from very long sparks an attractive possibility. The small size of the probe apparently causes negligible perturbation of the arc, even for approaches of a few centimeters.

Quantitatively, the radius-distance measurements shown in Figure 26 permit detailed analysis of the shock-flow field via Equations 4-1 to 4-6. Calculations of the overpressure, Mach number, normal-shock temperature jump, reflected-shock pressure and reflected-shock temperature are shown in Table VIII. The reflected-shock pressure jump $\frac{P_r}{P_o}$ is only 39 at 1 cm from the channel. Since the channel itself is of the order of 1 cm (Uman, 1969)[8] it is not reasonable to calculate conditions nearer the centerline. Thus, quite near the arc, even the reflected-shock pressure is relatively small. Consequently, the shock-heated air will exhibit a modest temperature jump and there will be negligible ionization. These calculations were made for the case of the 26,666 Joule arc in which 83 Joules are observed in the mechanical shock. Thus, the efficiency is less than one percent. If we speculate that natural electrical discharges are equally inefficient, lightning will typically be of

---

6. Jones, D.L. Faraday Rotation Measurements of the Precussor Ionization from an Exploding Wire Discharge, Exploding Wires, Vol. 4 (Plenum) 93, 1968b.

7. Uman, M.A., A.H. Cookson and J.B. Moreland, Shock Wave from a Four-Meter Spark, J. Appl. Phys., to be published June 1970.

8. Uman, M.A., Lightning, (McGraw-Hill) 35, 1969.

TABLE VIII

Shock Wave Parameters for Normal and Reflected Shocks

R(cm)	t(μs)	$\frac{P}{Po}$		$\frac{Pl}{Po}$	$\frac{Tl}{To}$	$\frac{Pr}{Po}$	$\frac{Tr}{To}$	T°k	Ne
1	34	7.5	2.7	8.5	2.4	39	4.0	1200	~1
2	45.8	2.2	1.6	3.2	1.5	9.7	2.1	630	
5	91	0.55	1.2	1.6	1.2	2.4	1		
10	231	0.27	1.1	1.3	1.1	1.6			
15	375	0.17	1.07	1.2		1.4			
20	520	0.13	1.05	1.13		1.3			
30	813	0.09	1.04	1.09		1.2			

the same magnitude in energy release (Jones et al. 1968). Consequently, the data presented in Table VIII may be a good representation of lightning effects. It would be helpful to run a series of properly controlled experiments on the very large arc to verify this conclusion.

In this study we have used the energy directly obtained from eqn (2). Plooster (1968), in a detailed analysis, shows that this procedure can lead to sizeable errors. We have evaluated this error and find it to be a maximum of 40 percent. An error of this magnitude is relatively unimportant to the conclusions developed. The dominant feature is rather the rapid damping of the shock, occasioned by the high pressure of the background air.

4.6 Conclusion

We have measured the trajectory of the open air spark and find it fits the theoretical cylindrical blast wave. Using the floating probe technique, we find it possible to make non-interacting measurements of shock waves to within a few centimeters of the 5,000,000 volt arc. Our results show that the atmospheric shock from the spark decays very rapidly and that shock produced ionization is negligible. The rapid decay of the shock probably explains the lack of shock damage to aircraft struck by lightning.

4.7 References

Few, A.A., Power Spectrum of Thunder, J. Geophys, Res. 74, 6926, 1969.

Few, A.A., H.B. Barrett, M.A. Uman, and L.E. Salanave, Comments on Letter by W.W. Troutman "Numerical Calculation of the Pressure Pulse from a Lightning Stroke" J. Geophys, Res. 1970.

Jones, D.L., Intermediate Strength Blast Wave, Phys. Fluids 11, 1664, 1968a.

Gilmore, F.R., Equilibrium Composition and Thermodynamic Properties of Air to 24,000°K, The Rand Corporation, Report Rm. 1543, August 1955.

Jones, T.G., and G.C. Vlases, Pressure Probes for Research in Plasma Dynamics and Detonation, Rev. Sco. Inst., 38, 1038, 1967

Uman, M.A., A.H. Cookson and J.B. Moreland, Shock Wave from a Four-Meter Spark, J. Appl. Phys., to be published June 1970.

Jones, D.L., Faraday Rotation Measurements of the Precussor Ionization from from an Exploding Wire Discharge, Exploding Wires, Vol. 4 (Plenum) 93, 1968b.

Uman, M.A., Lightning, (McGraw-Hill) 35, 1969.

Jones, D.L., G.G. Goyer and M,N. Plooster, Shock Wave from a Lightning Discharge, J. Geophys. Res., 73, 3121, 1968.

Plooster, M.N. Shock Waves from Line Sources, National Center for Atmospheric Research TN 37, 1968.

SECTION 5

5.0 - Investigator Services

The contract provided for a certain amount of time to be used to investigate accidents or incidents involving lightning flashes to aircraft. There was only one investigation of an incident involving an aircraft; this was made for an F-106 aircraft. Since there was a scarcity of lightning incidents to investigate, two other tasks were undertaken. The first of these involved the preparation of a questionnaire to be answered in the event of a lightning flash to an aircraft. The second task involved the preparation of a test plan covering work to be done on an F-4 aircraft to investigate the electrical transients produced by lightning striking this aircraft.

5.1 Lightning Incident Involving an F-106 Aircraft

At the time of the strike, the aircraft was within clouds at an altitude of 6500 feet, experiencing light turbulence. There was no precipitation, and no previous lightning flashes in the vicinity. The stroke that hit the aircraft was the only one observed. The pilot was not aware of any electrical activity before or after the strike. St. Elmo's fire was not observed before the stroke, but St. Elmo's fire is seldom observed except when it is dark.

Stroke Entrance and Exit Points

The pilot reported that the flash terminated on the radome in front of him. Apparently it did not strike the pitot boom on the front of the aircraft. Since the pitot boom was not found, and not available for inspection, the above observation could not be checked against any circumstantial evidence. If the flash did not involve the pitot boom, presumably the explosive shattering of the radome was not caused by explosion of the pitot boom heater wires. The stroke exited from the tail, a subject which will be expanded upon later.

Effects of the Stroke

General effects were as follows:

1) The two ac power systems for the radar were disabled while the two ac power systems for the aircraft remained on line.

2) There was no stiffening of controls and no engine flameout.

3) There were no adverse effects on the pilot, such as flash blindness and electrical shock.

4) As to avionics equipment damage, the radar was destroyed, but all of the UHF radios continued to function.

5) Structural damage to the nose of the aircraft was extensive. The entire radome canopy was blown off, the mounting ring for the radar was cracked at the top, and there were numerous panels dented or ripped, or that had torn rivets.

6) The access doors to the avionics compartment were blown loose. It is possible that they were blown off of the aircraft by the force of the explosion, but it is more likely that they were blown open by the blast and then torn loose from the aircraft by the wind buffeting.

Discussion of Effects

The damage to the nose section seems to have been produced by an explosive buildup of pressure within the nose section. It is difficult to estimate how much of the explosive energy came from arcing associated with the lightning current and how much came from products of combustion of the resulting fire. Arcing from the lightning flash could probably easily release enough energy in the confined nose section to produce the observed damage.

The evidence does indicate there was a fire caused by the lightning flash, but that this fire was of short duration.

The interior of the radome and avionic compartment was pretty well blackened. None of the wiring, however, showed signs of having been overheated or ripped by either high current flow or by the electromagnetic effects associated with the lightning flash.

The damage to electrical wiring seemed confined to surface discoloration (charring seems too strong a description) caused by a flash fire. There was extensive blackening of the middle structure in the nose section. The blackening again seems to be typical of a flash fire in that it is an oily residue. An oily residue would not be left by a purely electrical arc, hence this particular blackening is not of itself typical of a high amplitude short duration current discharge. Possibly there was an accumulation of hydraulic fluid or lubricating oil that could have burned, but this is mostly conjecture.

The structural damage that occurred seemed consistent with an explosion of some kind. Panels were bent, riveted joints torn loose, castings broken, etc. None of this damage would appear to be due to the electromagnetic motoring forces

caused by an interaction of a current-carrying member with the resultant magnetic fields.

Shattering of the fiberglass radome was typical of the flow of high current through a nonconductor. A given current will always release more energy when it arcs through a nonconducting or insulated member that when it flows through a structural member made of conductive metal. The instantaneous energy released is a product of the current that flows and the voltage drop along the conductor or arc path through which the current flows. In a conductive member, the resistance is low and hence the voltage drop is low. In an arc, the resistance is higher and the arc voltage drop is higher. If the arc goes across an insulating circuit, or if the arc is confined, the arc drop is higher still, hence leading to even more energy release. The more energy released, generally, the more mechanical damage that will be experienced.

Exactly where the arc terminated after puncturing the radome is difficult to say. The radome unit itself was not available for inspection, but the radar antenna, however, was completely shattered. Such shattering is typical of a high amplitude current discharge flowing through a nonconductor.

The exit point of the stroke was aft, through the vertical stabilizer at the junction of the metal portion of the stabilizer and the fiberglass section. The fiberglass was split, probably from the explosive effects of the point of current exit. At least some of the damage at the exit point was caused by sparking between the flat metal sheets of the stabilizer and the narrow metal trailing edge. These two pieces of metal were joined with an adhesive. Arcing took place through the adhesive with the typical, explosive shattering effect of an arc in a confined space. Probably part of the energy released was caused by the chemical burning of the adhesive. If damage of this nature consistently occurs, it would appear that it could be reduced by providing some sort of metal bonding to bridge this gap, possibly by means of several short beads of welding between the metal sheet and the trailing edge.

Arcing, and the resultant explosive release of gasses at the exit point, was probably also responsible for the splitting of the entire trailing edge of the upper section of the stabilizer, which was made of fiberglass. Possibly this damage could be avoided by a metal shield point between the parts of the stabilizer. This would provide a controlled arcing point, moving the arc point further away from the stabilizer and the fiberglass structures.

The burned area at the exit point seemed to be about 1" in diameter. No great amount of burned metal was visible, but the arc did wander around for about one or two inches forward of the extreme trailing point of the aircraft.

There was no real damage to the engine. There were a few nicked blades on the first stage of the compressor, but these could be repaired by grinding and they did not need to be removed from the engine. Two of the inlet screens were covered with fiberglass debris from the radome, but there was no engine flameout.

There were about six items of avionic equipment, from a panel containing 18 to 20 black boxes, that were damaged. These, of course, included the radar itself, this having been completely destroyed. Electronic equipment in other bays on the aircraft apparently was not damaged. Apparently there were no instances of sparking or other electrical effects within the cockpit of the aircraft. Quite possibly it would be feasible to stage arcing tests on this or a similar trailing edge structure to determine the total coulomb content of the lightning discharge.

As regards this particular incident, however, it seems unlikely that the knowledge obtained from such a test would warrant the cost of tests.

In summary then, it would appear that the discharge was a high amplitude discharge, possibly (though it is purely speculation) flashing from a cloud to the ground. The lack of extreme amounts of burned metal would indicate that the continuing current between strokes, if there was any, did not involve a large transfer of charge. In many respects, the structural damage is of the nature that one might expect if he were to pour a cup of gasoline into the enclosed area, mix it with sufficient air, and ignite the resultant vapor.

Figures 27, 28 and 29 show sketches of the resulting damage.

5.2 USAF Lightning Strike Report Form

A copy of a Lightning Strike Report form is shown on Figures 30 and 31. The information requested should allow a better analysis of lightning incidents than can now be made.

5.3 Test Plan for F-4 Aircraft

During the course of contract NAS3-12019, a portable test set has been developed that allows one to circulate current pulses of 100 - 1000 amperes through a

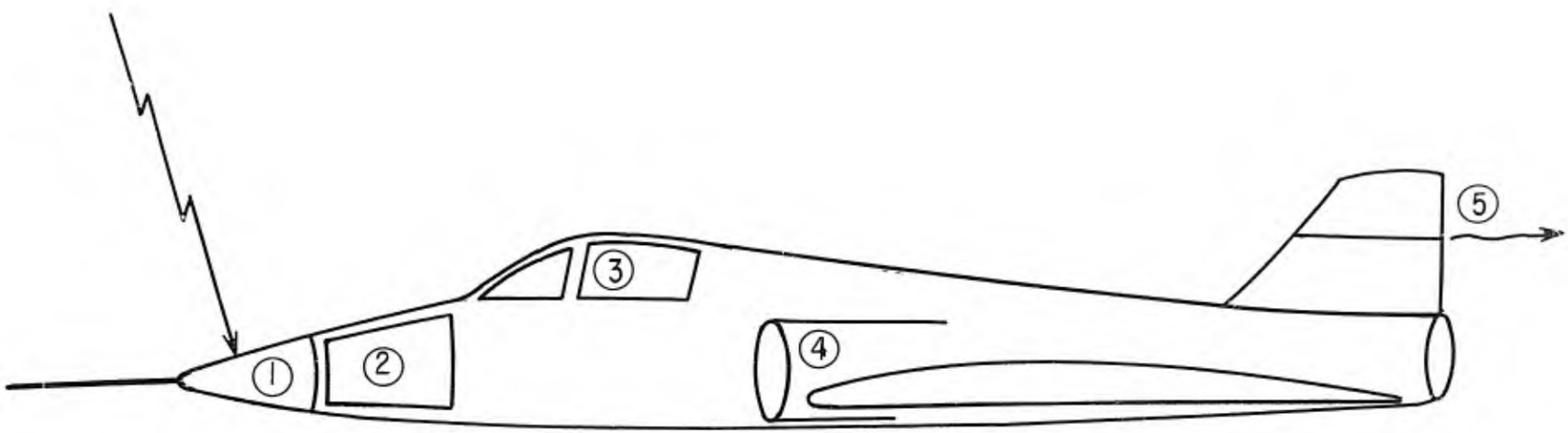

1) PILOTS OBSERVATION WAS THAT FLASH HIT TOP OF RADOME.
   RADOME WAS COMPLETELY BLOWN OFF, HENCE ACTUAL STROKE CONTACT POINT COULD NOT BE VERIFIED BY OBSERVATIONS OF DAMAGE.
2) EQUIPMENT BAY DOORS WERE BLOWN OFF, WITH CONSIDERABLE STRUCTURAL DAMAGE INTERNALLY.
3) NO ADVERSE EFFECTS WERE EXPERIENCED BY PILOT (NO ELECTRICAL SHOCK, FLASH BLINDNESS, ETC.)
4) NO REAL DAMAGE TO ENGINE.
5) EXIT POINT AT TAIL.

FIGURE 27

General Observations Regarding Lightning Flash to F106B Aircraft

1) RADAR MOUNTING RING CRACKED AND TWISTED OUT OF SHAPE.
2) SHEET METAL TORN AND BLOWN UP INTO EQUIPMENT BAY
3&4) BULKHEADS DENTED AND TORN; THESE WERE PUSHED TOWARDS REAR OF AIRCRAFT.
5) RADAR ANTENNA (NOT SHOWN) COMPLETELY DESTROYED.
6) BLACK AND OILY RESIDUE, PRESUMABLY FROM FLASH FIRE, ON WIRING AND METAL SURFACES.
7) EQUIPMENT BAY COVERS TORN LOOSE.
8) RADOME COMPLETELY GONE.

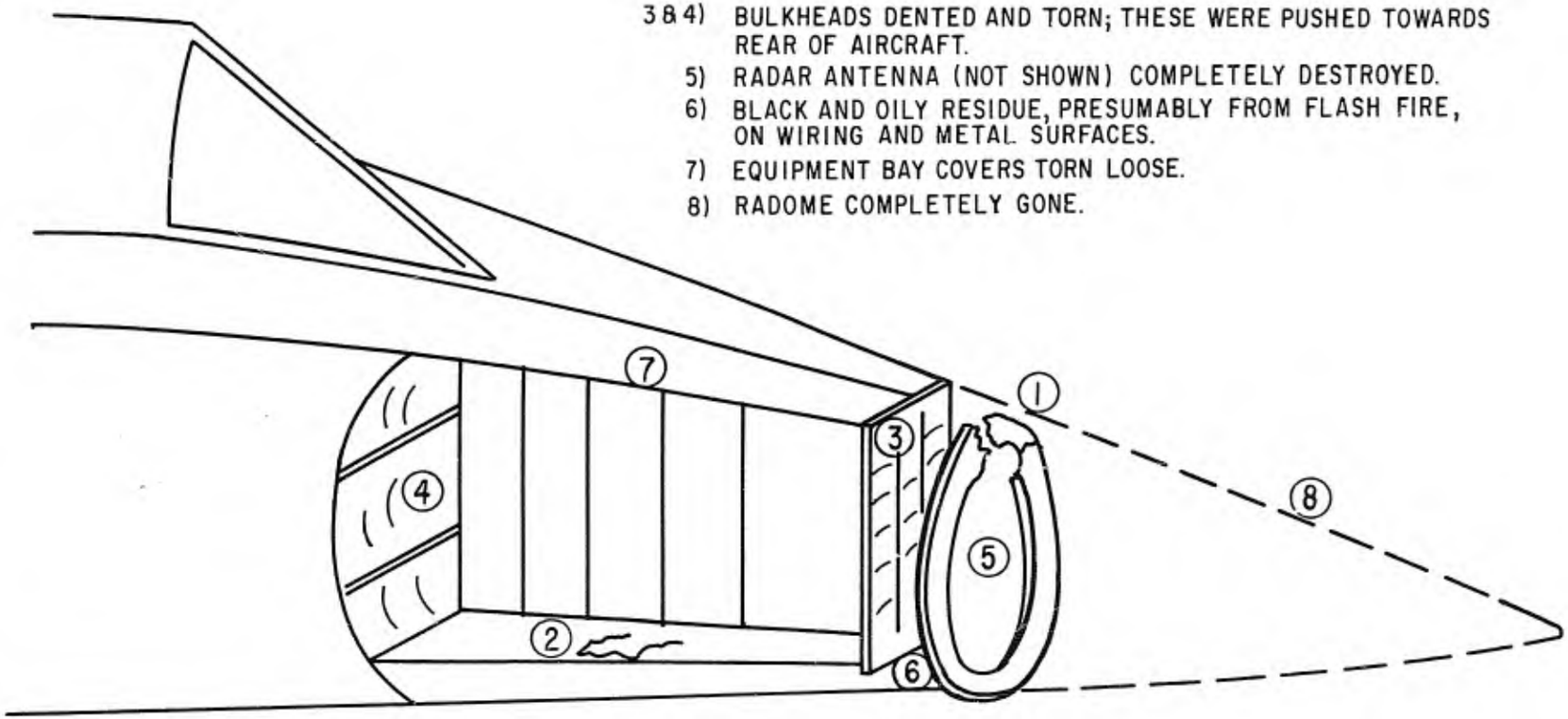

FIGURE 28

Lightning and Resulting Explosion Damage to Nose and Equipment Bay

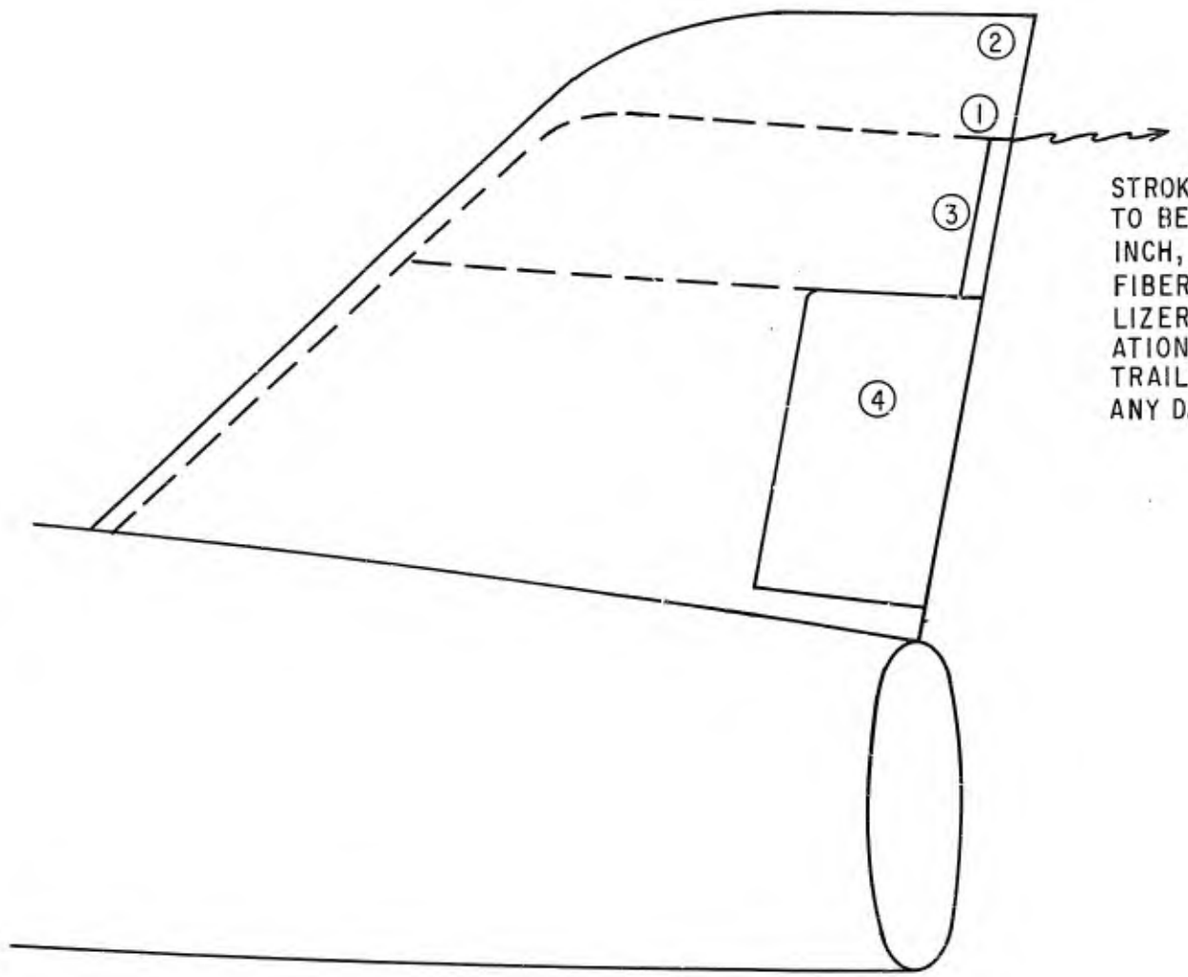

STROKE EXIT AT POINT (1) CAUSED METAL TO BE BURNT OVER APPROXIMATELY 1 SQ. INCH, CAUSED DELAMINATION OF THE FIBERGLASS UPPER SECTION OF THE STABILIZER (2). THIS CAUSED EXPLOSIVE SEPARATION OF THE ADHESIVE JOINT AT THE TRAILING EDGE (3), BUT DID NOT CAUSE ANY DAMAGE TO THE CONTROL SURFACE (4).

FIGURE 29

Conditions at Exit Point

USAF

LIGHTNING STRIKE REPORT

TO: AFAL (AVPT)

This report is to be completed and filed by the Air Crew following any flight during which lightning was known or believed to have struck the aircraft. The purpose of this report is to provide data to the Air Force Avionics Laboratory for use in support of its continuing research into the effects of lightning on aircraft. This research leads to the development of design criteria and measures for the protection of aircraft from the adverse effects of lightning. Operational experience data furnished by you on this form is extremely valuable in this effort.

INSTRUCTIONS

Please complete and file this report immediately following your flight, providing as much of the requested data as you can. Your visual observations of any unusual characteristics or damage suspected to be associated with lightning are especially important. It is recognized that not all of the following questions may be answerable. Please provide as much information, however, as possible, using estimates if exact figures are not known. If possible, please include with this report any photographs or snapshots of damaged parts, etc.

I. OPERATIONAL CONDITIONS AT TIME OF STRIKE

- Aircraft Type_____; Date_____; Time of Stroke _____
- Altitude _____ Ft; Air Speed _____ Kts; Condition _____ (Approach, climb, level flight, VFR, IFR, etc.)
- Mission_____
- Afterburner on? _____

II. ENVIRONMENTAL CONDITIONS AT TIME OF STRIKE

- Area Weather:

	Cloud Type	% Cover	Ceiling (ft.)	Tops at (ft.)	Precip. Type	Precip. %	Temp.
Forecast							
Actual							

- AT TIME OF STRIKE WAS AIRCRAFT: Within Cloud _____; Between Clouds_____; Above Clouds_____; Below Ceiling_____; Experiencing_____ Turbulence Experiencing Precip. in Form of_____.
- APPROX. HOW MANY LIGHTNING FLASHES DID YOU OBSERVE IN VICINITY? Before Aircraft was Struck_____, After Aircraft was Struck_____.
- WAS ST. ELMO'S FIRE PRESENT? _____ Where_____, How Long Prior to Strike_____
- DID YOU EXPECT A POSSIBLE STRIKE AT THIS TIME? _____
- OTHER COMMENTS _____

III. LIGHTNING STRIKE EFFECTS

- GENERAL DESCRIPTION: _____
- POINTS OF STROKE ATTACHMENT TO AIRCRAFT: (See also Part V) _____

(NOTE: A lightning stroke must always pass through the aircraft. Therefore, there will be at least two points of stroke attachment to the aircraft).

- Did stroke appear to sweep across/along surface of aircraft?_____

ELECTRICAL EFFECTS

- Describe any temporary interference or permanent damage effects of the stroke on any elements of the aircraft electrical or avionics systems:

STRUCTURAL EFFECTS

- Describe any structural damage believed to have occurred as a result of the lightning strike (See also Part IV)

Location of Holes Burned	Hole Dia. (In)	Skin Material	Skin Thickness

PERSONNEL EFFECTS

- Flash Blindness _____
- Electric Shock _____
- Other _____

OTHER EFFECTS

- Any effects on aircraft controllability?_____
  Temporary _____ Permanent_____
- Any unusual instrument readings before, during or after aircraft was struck? _____

Figure 3.0 - USAF LIGHTNING STRIKE REPORT - SECTIONS I, II, III

IV. TYPICALLY DAMAGED ITEMS

Aircraft components which often receive damage as a result of lightning strikes include the following items. It is well to check the condition of each of these following a strike.

- External Fuel Tanks
- External Armaments
- Engine Cowling
- Wing Tips
- Flaps and Ailerons
- Position Lamps
- Radome
- Canopy
- Pitot Tubes
- Nose or Tail Booms
- Nonmetallic Components
- Propellers
- Horizontal Stabilizer
- Vertical Stabilizer
- Rudder
- Tail Cone
- Antennas

V. SKETCHES OR OTHER DESCRIPTIONS OF LIGHTNING DAMAGE

Diagrams or sketches can be very helpful in providing an understanding of lightning phenomena. If you believe such an illustration would provide further clarity for this report, please use the following space for this purpose. Attach additional sheets if necessary.

VI. REPORT PREPARED BY: NAME_____

ORGANIZATION _____

Address/Phone No. where you can be contacted by the Avionics Laboratory for additional discussion.

ADDRESS_____ PHONE NO._____

Figure 3.1 - USAF LIGHTNING STRIKE REPORT - SECTION IV, V, VI

complete aircraft. The waveshape of the current pulses can be varied to cover the range of waveshapes representative of natural lightning stroke currents. The surge voltages induced on aircraft electrical circuits by these currents can be measured and then scaled up to the full threat levels of natural lightning. A portion of the contract work involved verification testing on an F-89 aircraft at the Naval Weapons Center in China Lake, California. During the course of this work, it was noticed that an F-4 aircraft was also located there. Recognizing that the F-4 aircraft has experienced more than its share of problems connected with lightning, we made arrangements to extend the electrical test series to include this particular aircraft. Work is currently in progress, and will be reported upon at a later date. In brief, this work involves:

1. Defining the most probable lightning current paths through the aircraft.

2. Establishing the specific electrical circuits and components which have been adversely affected by lightning so that the test plan gives priority to lightning-related problems already in existence. Examination of F-4 manuals indicated that there were 16 circuit types most likely to be involved in lightning events, and that these contained a total of 398 conductors. These are listed in Table IX.

3. Establishing the routing of these circuits and conductors in the aircraft in relationship to the probable stroke-attachment points and lightning current routes.

4. Measuring of the susceptibility of these circuits to lightning current passing through the aircraft.

5. Determining equivalent circuits that can be used to analytically relate lightning current to induced voltages.

TABLE IX

F-4 ELECTRICAL CIRCUITS SUSCEPTIBLE TO LIGHTNING

Circuit Identification Number	Description	Number of Conductors in Each Circuit
3	A-C Power Control	70
10	External Tanks Fuel Flow	12
27	Exterior Lights	25
31	Pitot Heater	7
34	Special Weapons Release	20
44	Stores Jettison	20
61	Radar Set AN/APQ-109	18
65	Flight Control Group	50
67	Tactical Air Navigation and Flight Director Group Subsystems	19
68	UHF Communications and ADF and Intercommunications Subsystems	30
70	Navigational Computer Set AN/ASN-46A	16
71	Air Data Computer Set	40
77	Bombs, Rockets, and CBU Release	45
86	Inertial Navigation Set AN/ASN-63	11
87	Electronic Counter-Measures System	10
98	Reel Launcher RMU-8 A Tow Target	5
	Total	398

SECTION 6

6.0 Summary of Parts I and II

Summarized results of the tests to determine the lightning resistance of boron and graphite test panels follow.

None of the salt-loaded or carbon black-loaded coatings screened for protective abilities showed any particular promise. In fact, most of the heavy coatings increased the damage to the test panel rather than decreasing it. All coatings seemed to confine the electrical arc to the interface between the coating and the panel, thus increasing the damage. Probably the damage results from a combination of two factors: 1) a confined arc will have a higher voltage drop per unit length, consequently releasing more energy per unit current and, 2) confining the arc increases the pressure buildup caused by the energy that is released. This confinement of pressure provides better mechanical coupling between the arc and the test panel, thus increasing the energy transfer into the panel and aggravating the damage.

Silver paint coatings on the 13" graphite test panels did not provide any significant lightning protection. There is some indication that they likewise increased the damage.

Flame-sprayed aluminum coatings provided better lightning protection, but not sufficient to provide protection at the 200 kA current level. The two coatings that showed good promise for lightning protection were the metal-plated coating on the 3" x 12" test samples and the aluminum mesh (Boeing development) on the honeycomb test sample supplied by Grumann. Coatings apparently have to be either highly conductive so as to carry high currents with low resistive voltage drop and hence low energy deposition in the coating, or must be highly insulating and able to keep lightning current out of the composite material. Only a metal coating can fulfill the first criteria. Apparently, quite thin metal coatings can carry very high currents as long as they are electrically continuous and there are no points at which sparking can occur between metal parts. Any time there is sparking across a joint, there is a high voltage drop and hence a high release of energy per unit of lightning current.

Dielectric coatings that promote a surface flashover may have some

application for aircraft protection, but probably only in a few situations. To be effective, a dielectric coating must have sufficient insulating strength that the arc voltage drop developed between the lightning stroke attachment point and the conductive metal ground point to which the surface flashover finally attaches does not lead to a puncture through the dielectric coating to the underlying composite material. In most cases, the required thickness of such dielectric coating would probably be too thick to be practical.

In principle, dielectric structures should be fairly resistant to the effects of lightning, as evidenced by the very minimal amounts of damage to the 3" x 12" fiberglass panels. In any application of dielectric structural members, the important consideration would be to insure that there is no conductive body underneath the dielectric material to which an arc can attach.

Composite materials themselves, whether graphite-based or boron-based, are neither sufficiently conductive to carry lightning currents without damage, nor sufficiently insulating to promote a surface flashover.

Tests of material properties made in the vicinity of the lightning stroke attachment point all seem to show that the intrinsic material damage caused by a lightning stroke did not extend very far beyond the point at which damage was visually evident. A rough rule of thumb would seem to indicate that material damage will be confined to a region of about twice the diameter of the area in which damage is visually evident.

Cracking or delamination between a composite skin and the underlying structural framework is a different story. Such cracking or delamination would be a function of the structural design of the system and not dependent on the current density within the bulk of the composite material.

Most of the nondestructive test techniques tried did not prove very successful in finding material damage that was not visually evident, largely because there did not seem to be much hidden damage to be found. Ultrasonic C-scans and x-ray extraction photographs did not show damage to the panels beyond that visually evident.

An attempt was made to use the sonic vibration patterns of the 13" circular panels before and after test to determine the regions damaged by

lightning current tests. This test technique again proved useless. Damage to the panels caused by the lightning current was sufficiently massive to destroy any particular vibration patterns that were evident before test.

In previous studies, resistance measurements have proven to be a good technique for showing whether individual strands or fibers of composite material were damaged by current flow. Resistance measurements on bulk sheets of composite material gave mixed results. On graphite panels, resistance measurements made between two points equally spaced gave about the same resistance whether they were made in an undamaged section of the panel or whether they were made diagonally across an area completely destroyed by a lightning stroke. Apparently the graphite is sufficiently conductive that current is carried through the entire panel and not through just the path directly between the resistance measurement probes. Accordingly, it would not appear that a resistive measurement on a graphite panel would show up hidden damage. On a boron panel, however, the resistive measurements were more effective in showing damage. Resistances between two points on opposite sides of a damaged area were an order of magnitude higher than corresponding resistance measurements made across an undamaged area. Presumably, resistance measurements might then indicate hidden damage in a boron panel. Resistance measurements might be more effective in determining damage to protective coatings. Resistances measured on one of the aluminum honeycomb panels to which a silver paint coating had been applied increased by about three orders of magnitude after the test panel was subjected to a high current discharge. Again, however, the damage to the coating by the lightning current was perfectly obvious to the unaided eye.

The nondestructive test technique that showed most promise was an acoustic impedance measurement. This is a test technique in which one acoustic transducer is used both to produce an acoustic signal and to receive the reflected acoustic signal and convert it into an electrical signal for display on the measurement apparatus. Accordingly, it is a one-side test that does not require access to both sides of the structure under test. It proved effective in correlating the areas of physical damage on the 13" test samples with the acoustic measurements. Presumably, it would be equally effective in locating cracks or delamination.

Photomicrographs of specimens adjacent to and removed from physically damaged areas of the boron and graphite panels showed the same pattern as regards hidden damage as did the nondestructive test techniques; namely, mechanical degradation of the basic composite material did not seem to extend very far beyond the area in which damage was evident to the unaided eye. Photomicrographs of graphite panels did not generally show any particular degradation of the graphite fibers other than tearing or blasting of the fibers in the vicinity of the arc-attachment point. Photomicrographs of boron fibers showed the characteristic kinds of damage noted during studies of individual boron fibers. It was evident that, as the current density in individual fibers reached a critical level, the tungsten substrate of the boron fiber was melted and fused together with the boron. Tests at different current levels showed good correlation between the amount of damage and the current. As the current was increased, damage that was initially confined to the surface plies eventually progressed into the panel to involve all the plies.

Photomicrographs showed that the mechanical damage to the material either involved physical lifting and tearing of the plies near the arc-attachment point or involved cracking transverse to the filaments in the individual plies. The photomicrographs seldom if ever showed evidence of cracks in which the individual fibers were torn apart axially to the fibers. Cracking transverse to the individual fibers would be expected, because the only resistance to such cracking would be the mechanical strength of the resins used to bind the fibers together.

The arc resistance tests did not really show any major effects due to ply orientation or to ply layup. Damage that was visually evident at the surface would typically be more pronounced in one direction than in the other direction, presumably because of the mechanical orientation of the fibers in the plies, but none of the tests showed that any individual ply carried substantially more or less current than other plies. There seems to be sufficient electrical contact between the various plies that the panels behave electrically as homogeneous materials. This lack of ply effect, or apparent electrical homogeneity of the panels, was also observed during low-level current injection tests. Tests at low-current levels, of the order of 100 amperes, did not show any indication of sparking or

electrical breakdown between the various plies of test panels. Even resistance measurements made at levels of a few volts showed that all of the plies were electrically interconnected. Since the plies were well interconnected electrically, any current injected into the center of the test panel divided pretty equally among all the different plies and among the different axes of the test panel. In some cases nonuniform division of current was noted, but in all cases this seemed to be due to the orientation of the electrical connections from the surge generator to the panel. All of the indications are that the flow of current in a composite material will be determined more by the external electromagnetic field orientation caused by the lightning stroke than by the properties of the composite material itself.

The tests on the aircraft lightning arresters showed that significant amounts of current can be drawn through the arrester during the predischarge phase of a lightning stroke, or during that period in which the lightning flash is developing and approaching the aircraft, but before the actual high current discharge to the aircraft actually takes place. Currents of one to 100 amperes can be drawn from protruding objects on the aircraft solely by the high electric field associated with a developing lightning stroke. These currents can flow for several microseconds prior to actual contact of the high voltage or high current lightning discharge to the aircraft. The tests, in fact, indicated that whenever the electric field strength on the surface of the aircraft approaches 100,000 volts per meter, there will be discharges from protruding objects on the aircraft. These discharges will tend to limit the electrical field strength at the surface of the aircraft to around 100,000 volts per meter. Limitation of an electrical field strength at the surface of the aircraft to about 100,000 volts per meter helps define the electrical environment to which electrical apparatus within the aircraft will be subjected. In metal aircraft the structure of the aircraft inherently provides extremely good shielding against a high impedance electric field. If composite materials are used for aircraft, they will not provide as effective shielding against the electric field.

Since predischarge currents can flow from an aircraft antenna for several microseconds prior to actual contact of the lightning stroke, it would appear that aircraft lightning arresters should not be tested with an applied voltage that rises too rapidly.

The tests showed that the predischarge currents drawn from protruding points on an aircraft (antennas being such a protruding point) are not quasi-continuous currents, but come in a series of current bursts, each of fairly short duration lasting less than one microsecond. These individual bursts of current will be passed through the arrester to the connected avionic equipment. The voltage developed on the avionic equipment by these pulses of current will be determined in large measure by the impedance characteristics of the connected avionics load. A given pulse of current will produce more voltage across a high impedance load than across a low impedance load. Voltages produced across a tuned circuit load will be oscillatory in nature and of an amplitude determined by the capacitance of the tuned circuit and the Q-factor of the tuned circuit. Associated currents will be passed until such time as the integrated magnitude of the predischarge current builds up sufficient voltage across the blocking capacitor of the lightning arrester to trigger a flashover of the arrester's discharge gap. Only after the arrester gap flashes over will there by any voltage limiting action caused by the lightning arrester. The design of the avionic equipment should reflect the fact that significant amounts of charge can be passed through an arrester before the arrester becomes effective.

As expected, measurements of the electromagnetic shielding properties of composite materials showed that they will provide much less shielding than metal structures. An attempt was made to measure electromagnetic field transfer through the panels simultaneously with the application of the lightning currents used to determine the ability of panels to withstand such currents. These measurements proved not to be very useful, however. The lightning current discharge waveforms were predominantly of low frequency, frequency components greater than 500 kHz being of negligible amplitude.

The intrinsic shielding effectiveness of the panels under test was only one or two dB at this frequency. In addition, the impedance of the electromagnetic field produced at the surface of the panel by the flow of lightning current on the surface of the panel was not consistent or controllable. Accordingly, the use of high level pulse fields to evaluate shielding effectiveness was discontinued early in the test series; instead,

continuous wave or discrete frequency measurements were made. These gave more meaningful and consistent test results. The measurements showed that boron panels had much less intrinsic shielding effectiveness than did graphite panels and that, in any case, the shielding effectiveness of the panels was inferior to the conductive coatings that might be used on the panels. As examples, at a frequency 5 MHz, a 0.083" thick boron-based panel had a shielding effectiveness of about 7 dB as contrasted to 19 dB provided by a 0.083" graphite-based panel. By contrast, a flame-sprayed aluminum coating on either the boron or graphite based panels yielded a total shielding effectiveness of about 35 dB at the 5 MHz frequency. Two other graphite test panels of different size gave comparable results. A 0.040" graphite panel had a shielding effectiveness of about 7 dB at 5 MHz, whereas a 0.120" graphite panel had about 19 dB shielding effectiveness. A 3-mil coating of silver paint on these latter graphite panels raised the shielding effectiveness by only one dB, considerably less than the flame-sprayed aluminum did on the boron and graphite based panels. None of the panels had anything like the shielding effectiveness of a solid metal sheet. For example, even a 1.6 mil thickness of aluminum foil at 5 MHz had a shielding effectiveness of about 43 dB.

Five MHz represents about the upper level of frequency contained in a high amplitude lightning current discharge waveform. As is typical of most shielding materials, shielding effectiveness is less at lower frequencies. At frequencies below one MHz, both boron and graphite panels of all the thicknesses tested had shielding effectivenesses of less than 10 dB.

Shielding effectiveness measurements were not made above 30 MHz, but the data obtained during this contract does line up well with that obtained by other investigators at frequencies of up to 400 MHz.

The implications regarding electromagnetic interference problems associated with lightning are clear. Composite materials by themselves should not be relied upon to provide any shielding. Any shielding properties must come from metal protective coatings on the composite materials rather than from the materials themselves. Design practices relating to routing of wiring or protection of avionic equipment derived from experience on metal aircraft will not be applicable to future aircraft making extensive use of composite materials. Whereas in the past structural design groups have

provided electromagnetic shielding for electrical circuits as an unintentional by-product of their efforts, they can not do so in the future. Shielding and overvoltage protection for all electrical circuits will have to be carefully considered by electrical design groups. Just as electromagnetic compatibility will be more of a problem in the future as regards the low-level electromagnetic environment caused by the various pieces of avionic equipment, so will there be more of a problem as regards the extremely high-level electromagnetic interference produced by lightning activity. Control of the electromagnetic interference problems associated with lightning can be provided through judicious cable routing, the use of cable shielding, and/or overvoltage protection devices, but these means of minimizing electromagnetic interference problems will have to be factored into the initial design stages of nonmetal aircraft. If electrical design groups ignore an interference problem or try to extrapolate it only from their experience on past generations of metal aircraft, the possibility exists of a serious retrofit or redesign phase on future generations of any aircraft making extensive use of composite materials for structural purposes.

Measurements in the vicinity of an electrical arc through a simulated aircraft structure have indicated that the electric field strength at the surface of an aircraft is unlikely to exceed about 100,000 volts per meter, at least on smooth or flat sections of the aircraft skin. Those measurements, however, did not indicate anything of the spectral content of the electromagnetic field associated with a lightning stroke. However, in an attempt to relate spectral content to the frequency of observation, additional measurements were made in the vicinity of a long electrical arc. The data was not completely conclusive, particularly at the low frequency end of the spectrum where attenuator failure and oscillations of the external impulse circuit may have affected results. Over the general range of 1 MHz to 1000 MHz, measurements seemed reasonably consistent and indicated that the energy radiated from a high voltage arc decreases at a 1/f rate out to approximately 100 MHz; then it falls off at a faster rate. The character of the radiation was definitely associated with the physics of the generation of the high voltage arc. At low frequencies, electric fields were produced as much by the current flowing in the impulse generator circuit producing the arc as by the arc itself. When resolved by time, the

electromagnetic fields at low frequencies were not produced until such time as the electrical arc was fully developed and current was flowing in the entire arc-generator test circuit. At higher frequencies, however, significant amounts of radiation were detected even before the arc was developed. These were associated with the predischarge portion of the developing electrical arc. In an actual lightning flash, one would expect significant amounts of electrical radiation from the developing lightning flash even before it struck the aircraft.

Virtually all the measurements made were measurements of the electric field. A few measurements were made of the magnetic field (using a loop antenna as contrasted to a rod antenna) in the range of 1 MHz to 20 MHz. These generally gave field strengths several dB lower than the comparable measurements of electric field strength. This would indicate that the field being measured had an impedance higher than the 377 ohms associated with plane wave propagation through free space. In the vicinity of an electrical arc, the radiation characteristics of the field are those determined by the near-field coupling mechanisms between the energy source and the object being affected by the field. These impedance relations can be very complicated; therefore, one should never assume that the electric and magnetic field strengths are related by the 377 ohms associated with plane wave propagation. As a rather extreme example, but nevertheless a very practical one, at the surface of a metallic aircraft the electric field strength will fall to zero while the magnetic field strength remains high. This corresponds to a low impedance field condition. The shielding effectiveness of structural materials, of course, depends strongly on the impedance of the field against which one is trying to provide shielding. In general, it would seem appropriate to concentrate attention to the low impedance fields associated with the flow of lightning current on the aircraft skin or the flow of lightning current at the stroke-attachment point.

Measurements of acoustic pressures in the vicinity of a high voltage electrical spark led to the conclusion that less than one percent of the energy stored in the capacitance of an impulse generator was coupled into the mechanical shock wave associated with the high voltage arc produced when the generator discharged. The overpressure associated with the shock wave from the electrical arc was relatively low and decayed quickly to an

ambient value. On the assumption that lightning behaves in a similar way, this would indicate the lack of shock damage to structures hit by lightning, since only a small fraction of the total energy would be mechanically coupled into the shock wave propagating in the surrounding air. Pressure buildup from confined arcs was not examined during this contract. Whenever an arc is confined, the arc voltage will rise and a given current will produce more energy deposition in the arc. This leads to increased temperatures and increased blast pressures. Further research on the mechanism of coupling of electrical energy in the lightning stroke channel into mechanical energy and the resultant damage to mechanical structures might be a subject for consideration as a future research project.

Relative to investigations of aircraft incidents and accidents caused by lightning, only one investigation was made during the course of this contract. This involved a lightning stroke to an F-106 aircraft which did not cause loss of the aircraft, but did cause sufficient mechanical damage to the aircraft as to elevate the status from a lightning incident to a lightning-caused accident. A summary of the results of the investigation are contained in the body of the report.

"PRECEDING PAGE BLANK-NOT FILMED."

Distribution
not Shot

Unclassfied

Security Classification

DOCUMENT CONTROL DATA - R & D

(Security classification of title, body of abstract and indexing annotation must be entered when the overall report is classified)

1. ORIGINATING ACTIVITY (Corporate author)	2a. REPORT SECURITY CLASSIFICATION
General Electric Company High Voltage Laboratory Pittsfield, Mass.	Unclassified
	2b. GROUP

3. REPORT TITLE

Lightning Effects Relating to Aircraft
Part II - Characteristics of Simulated Lightning Flashes and Their Effects on Lightning Arresters and Avionic Equipment

4. DESCRIPTIVE NOTES (Type of report and inclusive dates)

Final Report for the period 15 Nov 69 to 15 Jan 72

5. AUTHOR(S) (First name, middle initial, last name)

F.A. Fisher, B. Macchiaroli, D.L. Jones

6. REPORT DATE	7a. TOTAL NO. OF PAGES	7b. NO. OF REFS
15 January 1972	107	15

8a. CONTRACT OR GRANT NO.	9a. ORIGINATOR'S REPORT NUMBER(S)
F33615-70-C-1144	
b. PROJECT NO. 6091	SRD-72-054-II
c.	9b. OTHER REPORT NO(S) (Any other numbers that may be assigned this report)
d.	AFAL-TR-72-5

10. DISTRIBUTION STATEMENT Distribution limited to US Government agencies only for reason of test and evaluation, dated January 1972; other requests for this document must be referred to AFAL/AAA, Wright-Patterson AFB, Ohio.

11. SUPPLEMENTARY NOTES	12. SPONSORING MILITARY ACTIVITY
	Air Force Avionics Laboratory Air Force Systems Command Wright-Patterson Air Force Base, Ohio

13. ABSTRACT

Measurements were made of the degree to which a lightning arrester could limit the voltage on avionic equipment when an external lightning arrester was struck by a simulated lightning stroke. The tests show that breakdown is not an instantaneous affair, but rather takes many microseconds. Measurements taken near a point which is struck indicate that the air around any protrusions will be in a state of electrical breakdown whenever the electrical field strength at the aircraft surface approaches 100 kV/Meter. Electrical discharges tend to limit the field strength to that value, thus defining the electrical environment to which the avionics equipment is subjected. Data is presented showing how the impedance affects the voltages impressed on avionic equipment before the spark gaps in the protecting lightning arrester break down.

Measurements were made of the spectral density of radiation from long electrical arcs used to simulate lightning strokes to aircraft. The relative amplitude at different frequencies seems to agree with that observed from natural lightning, falling at 1/f rate in the vicinity of 1 MHz.

DD FORM 1 NOV 65 1473

Unclassified

Security Classification

KEY WORDS	LINK A		LINK B		LINK C	
	ROLE	WT	ROLE	WT	ROLE	WT
Lightning Effects						
Lightning Arresters						
Electromagnetic Interference						
Shock Waves						
Electrical Arcs						
Avionic Equipment						
Predischarge Currents						

END 7-72